and GII/15). A third contained two genotypes (i.e., GI/5 and GII/15), and the last also contained two genotypes (i.e., GII/5 and GII/15). GII15 was a common genotype. As many as eight genotypes were detected in those outbreaks.

Single genotypes were observed in most outbreaks that occurred in semiclosed communities, such as dormitories, nursing homes, schools, and nursery schools. In outbreak 199906, all five NV-positive stool samples contained a common genotype, GII/5. Similarly, all four specimens in outbreaks 199811 and 199914 contained GII/3 and GII/6, respectively, and all three specimens in 200240 contained GII/2.

Surprisingly, many genotypes were found in the Saitama area in the past 5 years. Although they are from 156 stool specimens within the 66 outbreaks, we identified 26 of 31 genotypes. Only five genotypes (i.e., GI/6, GI/10, GII/9, GII/13, and GII/17) were not observed.

Genogrouping and genotyping. Real-time RT-PCR detected and distinguished genogroups GI and GII and has proved itself a useful screening method. Genogrouping based on this method was confirmed in all specimens by genotyping with phylogenetic analysis of RT-PCR products (Table 1). For example, stool specimen KU82 appeared to contain both GI and GII by real-time RT-PCR, and GI/2, GI/4, GI/5, and GII/15 were actually detected by genotyping. In the case of KU4, only GI was detected by real-time RT-PCR, and GI/1 and GI/7 were identified by RT-PCR after sequencing analysis. In the case of T28, only GII was detected, and the specimen contained three genotypes, GII/1, GII/4, and GII/9 (Table 1).

DISCUSSION

In this study, we used real-time RT-PCR plus electron microscopy to screen NV in stool specimens from 66 outbreaks in the Saitama area. The real-time RT-PCR method greatly saved the time required for selecting stool specimens for further analysis. From 156 NV-positive specimens, we obtained 368 capsid N/S gene sequences after cloning the RT-PCR products that were amplified with primer sets GIFF/GISKR and G2FB/G2SKR (18). Genotyping was performed by phylogenetic analyses according to the scheme described previously (19).

We note that all shellfish-related outbreaks were caused by multiple NV genotypes (Table 1). With their filter-feeding mechanisms, shellfish, such as oysters, can concentrate NV from an environment contaminated by multiple genotypes. In fact, oysters in the markets were found to contain several different genotypes (data not shown). Furthermore, some outbreaks displayed multiple genotypes with relatively high frequencies; the outbreaks occurring in 67% of private homes, 56% of restaurants, 33% of hotels, and 13% of catered lunches were strongly suspected to be due to shellfish. For example, shellfish were the common source for outbreak 199917 (Table 1). In this outbreak, specimens were obtained from four patients, and each specimen contained multiple genotypes, but the genotypes did not coincide with each other except for GII/15. Also, for example, in outbreak 200126, three specimens contained multiple genotype strains, but a common genotype strain did not exist (Table 1).

Among outbreaks which were not directly related to shellfish, there were some in which multiple genotypes were detected. In outbreak 199921 involving a restaurant but not shellfish, multiple genotypes were identified. One specimen (KU105) contained three genotypes (GI/4, GII/4, and GII/6), two specimens (KU109 and KU111) contained two genotypes (GI/4 and GII/6), and another specimen (KU112) contained only one genotype (GI/4). In this outbreak, the four individuals had eaten dinner together. Since no common foods, such as oysters, were identified, the cook, from whom KU115 was collected, was presumed to be the source. KU115 contained one genotype, GI/4, that was a common genotype in this outbreak. Other genotypes were not detected from this specimen. However, the cook was tested for NV long after the other patients were tested. Possibly, in the early stage of the disease, the cook had shed at least all three genotypes (GI/4, GII/4, and GII/6) and transmitted them to the other individuals by poor handling of cooked food. At a later stage, perhaps the virus titers in KU115 were lower, and only the predominant genotype GI/4 was detected. Also, in outbreak 200138, at school, multiple genotypes (GII/4 and GII/5) were also identified in one of three specimens. The other two specimens contained only a common genotype (GII/5) (Table 1).

On the other hand, stool specimens from outbreaks in semiclosed communities contained only single genotypes, with the exception of outbreak 200138. Fourteen of 66 outbreaks occurred in semiclosed communities (schools, nursery schools, nursing homes, and dormitory), and only seven genotypes (i.e., GI/3, GI/4, GII/2, GII/3, GII/4, GII/5, and GII/6) were found. In each outbreak, one genotype was likely transmitted through the fecal-oral route.

In NV infection, individual patients seem to differ in their susceptibility to each genotype. We confirmed that the genotypes which we identified were also antigenically distinct by an antigen enzyme-linked immunosorbent assay with hyperimmune sera against virus-like particles (unpublished data). Thus, susceptibility to each genotype seems to differ in each individual, perhaps due to differences in acquired immunity from previous NV infections. The different susceptibilities may also be due to specific ABO histo-blood group antigens in each individual, as described in recent studies (12-14, 25).

Furthermore, in the case of person-to-person infection with NV, selection of strains may occur during sequential passages in the outbreak due to the factors on the agent side, such as pathogenicity, reproductive rate in the host, and/or stability in the environment. When a person is infected first by multiple genotype strains, a strain that replicates faster and has greater stability may eventually become predominant later in the outbreak. Further epidemiological investigation may be necessary to clarify the mechanism of selection.

In the present study, we classified NV into 31 distinct genotypes (Fig. 1). This analysis added five GI and seven GII genotypes to the previously published list (19), and all of these new genotypes, except for GII/9 and GII/13, were detected in the Saitama area. GII/10 and GII/14 were isolated exclusively in Germany and the United States. In the Saitama area during the study period, a total of 26 of the 31 genotypes, including 10 new genotypes, were found. Saitama Prefecture is only 3,800 km^2 and $\approx$1% of the total area of Japan. It is surprising that this small region contained such a diversity of genotypes, including ones found in North and South America, Europe, Oceania, and Asia (Fig. 1). The extensive diversity in the Saitama area suggests that many genotypes were imported

from and exported to other countries with NV-contaminated foods and travelers afflicted with NV. Various genotypes of NV may be circulating around the world, and more new genotypes are likely to be discovered in the future.

With a combination of screening by real-time RT-PCR and genotyping by phylogenetic analysis, detection of NV in sewage, rivers, seawater, and foods may improve our understanding in the epidemiology of NV and, in turn, help us to prevent and control future NV outbreaks.

ACKNOWLEDGMENTS

We thank Sakae Inouye (Otsuma Women's University, Japan) for critical review of the manuscript.

This work was supported by Research in Health Sciences Focusing on Drug Innovation grant KH51048 from the Japan Health Sciences Foundation.

REFERENCES

1. **Ando, T., S. S. Monroe, J. R. Gentsch, Q. Jin, D. C. Lewis, and R. I. Glass.** 1995. Detection and differentiation of antigenically distinct small round-structured viruses (Norwalk-like viruses) by reverse transcription-PCR and Southern hybridization. J. Clin. Microbiol. **33**:64–71.
2. **Berke, T., B. Golding, X. Jiang, D. W. Cubitt, M. Wolfaardt, A. W. Smith, and D. O. Matson.** 1997. Phylogenetic analysis of the Caliciviruses. J. Med. Virol. **52**:419–424.
3. **Caul, E. O., and H. Appleton.** 1982. The electron microscopical and physical characteristics of small round human fecal viruses: an interim scheme for classification. J. Med. Virol. **9**:257–265.
4. **De Leon, R., S. M. Matsui, R. S. Baric, J. E. Herrmann, N. R. Blacklow, H. B. Greenberg, and M. D. Sobsey.** 1992. Detection of Norwalk virus in stool specimens by reverse transcriptase-polymerase chain reaction and nonradioactive oligoprobes. J. Clin. Microbiol. **30**:3151–3157.
5. **Felsenstein, J.** 1985. Confidence limits on phylogenies: an approach using the bootstrap. Evolution **39**:783–791.
6. **Glass, P. J., L. J. White, J. M. Ball, I. Leparc-Goffart, M. E. Hardy, and M. K. Estes.** 2000. Norwalk virus open reading frame 3 encodes a minor structural protein. J. Virol. **74**:6581–6591.
7. **Glass, R. I., J. Noel, T. Ando, R. Fankhauser, G. Belliot, A. Mounts, U. D. Parashar, J. S. Bresee, and S. S. Monroe.** 2000. The epidemiology of enteric caliciviruses from humans: a reassessment using new diagnostics. J. Infect. Dis. **181**(Suppl. 2):S254–S261.
8. **Green, K. Y., A. Z. Kapikian, and R. M. Chanock.** 2001. Human caliciviruses, p. 841–874. *In* D. M. Knipe, P. M. Howley, D. E. Griffin, et al. (ed.), Fields virology, 4th ed. Lippincott-Raven, Philadelphia, Pa.
9. **Green, S. M., P. R. Lambden, E. O. Caul, and I. N. Clarke.** 1997. Capsid sequence diversity in small round structured viruses from recent UK outbreaks of gastroenteritis. J. Med. Virol. **52**:14–19.
10. **Green, S. M., P. R. Lambden, Y. Deng, J. A. Lowes, S. Lineham, J. Bushell, J. Rogers, E. O. Caul, C. R. Ashley, and I. N. Clarke.** 1995. Polymerase chain reaction detection of small round-structured viruses from two related hospital outbreaks of gastroenteritis using inosine-containing primers. J. Med. Virol. **45**:197–202.
11. **Hafliger, D., M. Gilgen, J. Luthy, and P. Hubner.** 1997. Seminested RT-PCR systems for small round structured viruses and detection of enteric viruses in seafood. Int. J. Food Microbiol. **37**:27–36.
12. **Harrington, P. R., L. Lindesmith, B. Yount, C. L. Moe, and R. S. Baric.** 2002. Binding of Norwalk virus-like particles to ABH histo-blood group antigens is blocked by antisera from infected human volunteers or experimentally vaccinated mice. J. Virol. **76**:12335–12343.
13. **Hutson, A. M., R. L. Atmar, D. Y. Graham, and M. K. Estes.** 2002. Norwalk virus infection and disease is associated with ABO histo-blood group type. J. Infect. Dis. **185**:1335–1337.
14. **Hutson, A. M., R. L. Atmar, D. M. Marcus, and M. K. Estes.** 2003. Norwalk virus-like particle hemagglutination by binding to histo-blood group antigens. J. Virol. **77**:405–415.
15. **Inouye, S., K. Yamashita, S. Yamadera, M. Yoshikawa, N. Kato, and N. Okabe.** 2000. Surveillance of viral gastroenteritis in Japan: pediatric cases and outbreak incidents. J. Infect. Dis. **181**(Suppl. 2):S270–S274.
16. **Jiang, X., P. W. Huang, W. M. Zhong, T. Farkas, D. W. Cubitt, and D. O. Matson.** 1999. Design and evaluation of a primer pair that detects both Norwalk- and Sapporo-like caliciviruses by RT-PCR. J. Virol. Methods **83**: 145–154.
17. **Jiang, X., M. Wang, D. Y. Graham, and M. K. Estes.** 1992. Expression, self-assembly, and antigenicity of the Norwalk virus capsid protein. J. Virol. **66**:6527–6532.
18. **Kageyama, T., S. Kojima, M. Shinohara, K. Uchida, S. Fukushi, F. B. Hoshino, N. Takeda, and K. Katayama.** 2003. Broadly reactive and highly sensitive assay for Norwalk-like viruses based on real-time quantitative reverse transcription-PCR. J. Clin. Microbiol. **41**:1548–1557.
19. **Katayama, K., H. Shirato-Horikoshi, S. Kojima, T. Kageyama, T. Oka, F. Hoshino, S. Fukushi, M. Shinohara, K. Uchida, Y. Suzuki, T. Gojobori, and N. Takeda.** 2002. Phylogenetic analysis of the complete genome of 18 Norwalk-like viruses. Virology **299**:225–239.
20. **Kimura, M.** 1980. A simple method for estimating evolutionary rates of base substitutions through comparative studies of nucleotide sequences. J. Mol. Evol. **16**:111–120.
21. **Kobayashi, S., K. Sakae, Y. Suzuki, H. Ishiko, K. Kamata, K. Suzuki, K. Natori, T. Miyamura, and N. Takeda.** 2000. Expression of recombinant capsid proteins of chitta virus, a genogroup II Norwalk virus, and development of an ELISA to detect the viral antigen. Microbiol. Immunol. **44**:687–693.
22. **Kojima, S., T. Kageyama, S. Fukushi, F. B. Hoshino, M. Shinohara, K. Uchida, K. Natori, N. Takeda, and K. Katayama.** 2002. Genogroup-specific PCR primers for detection of Norwalk-like viruses. J. Virol. Methods **100**: 107–114.
23. **Liu, B., I. N. Clarke, and P. R. Lambden.** 1996. Polyprotein processing in Southampton virus: identification of 3C-like protease cleavage sites by in vitro mutagenesis. J. Virol. **70**:2605–2610.
24. **Liu, B. L., I. N. Clarke, E. O. Caul, and P. R. Lambden.** 1995. Human enteric caliciviruses have a unique genome structure and are distinct from the Norwalk-like viruses. Arch. Virol. **140**:1345–1356.
25. **Marionneau, S., N. Ruvoen, B. Le Moullac-Vaidye, M. Clement, A. Cailleau-Thomas, G. Ruiz-Palacois, P. Huang, X. Jiang, and J. Le Pendu.** 2002. Norwalk virus binds to histo-blood group antigens present on gastroduodenal epithelial cells of secretor individuals. Gastroenterology **122**:1967–1977.
26. **Matson, D. O., W. M. Zhong, S. Nakata, K. Numata, X. Jiang, L. K. Pickering, S. Chiba, and M. K. Estes.** 1995. Molecular characterization of a human calicivirus with sequence relationships closer to animal caliciviruses than other known human caliciviruses. J. Med. Virol. **45**:215–222.
27. **Moe, C. L., J. Gentsch, T. Ando, G. Grohmann, S. S. Monroe, X. Jiang, J. Wang, M. K. Estes, Y. Seto, C. Humphrey, et al.** 1994. Application of PCR to detect Norwalk virus in fecal specimens from outbreaks of gastroenteritis. J. Clin. Microbiol. **32**:642–648.
28. **Noel, J. S., T. Ando, J. P. Leite, K. Y. Green, K. E. Dingle, M. K. Estes, Y. Seto, S. S. Monroe, and R. I. Glass.** 1997. Correlation of patient immune responses with genetically characterized small round-structured viruses involved in outbreaks of nonbacterial acute gastroenteritis in the United States, 1990 to 1995. J. Med. Virol. **53**:372–383.
29. **Noel, J. S., R. L. Fankhauser, T. Ando, S. S. Monroe, and R. I. Glass.** 1999. Identification of a distinct common strain of "Norwalk-like viruses" having a global distribution. J. Infect. Dis. **179**:1334–1344.
30. **Saitou, N., and M. Nei.** 1987. The neighbor-joining method: a new method for reconstructing phylogenetic trees. Mol. Biol. Evol. **4**:406–425.
31. **Stene-Johansen, K., and B. Grinde.** 1996. Sensitive detection of human Caliciviridae by RT-PCR. J. Med. Virol. **50**:207–213.
32. **Thompson, J. D., T. J. Gibson, F. Plewniak, F. Jeanmougin, and D. G. Higgins.** 1997. The CLUSTAL_X windows interface: flexible strategies for multiple sequence alignment aided by quality analysis tools. Nucleic Acids Res. **25**:4876–4882.
33. **Vinje, J., S. A. Altena, and M. P. Koopmans.** 1997. The incidence and genetic variability of small round-structured viruses in outbreaks of gastroenteritis in the Netherlands. J. Infect. Dis. **176**:1374–1378.

Novel Recombinant Sapovirus

Kazuhiko Katayama,* Tatsuya Miyoshi,† Kiyoko Uchino,† Tomoichiro Oka,* Tomoyuki Tanaka,† Naokazu Takeda,* and Grant S. Hansman*‡

We determined the complete genome sequences of two sapovirus strains isolated in Thailand and Japan. One of these strains represented a novel, naturally occurring recombinant sapovirus. Evidence suggested the recombination site was at the polymerase-capsid junction within open reading frame one.

The positive-sense polyadenylated single-stranded RNA virus family *Caliciviridae* contains four genera, *Norovirus*, *Sapovirus*, *Lagovirus*, and *Vesivirus* (1). Human norovirus is the most important cause of outbreaks of gastroenteritis in the United States and infects all age groups (2). Human sapovirus is also a causative agent of gastroenteritis but is more frequent in young children than in adults (3). Most animal caliciviruses are grouped within the other two genera. In 1999, Jiang et al. (4) identified the first naturally occurring human recombinant norovirus, and several other strains were later described as recombinants (5 8). Evidence suggested that the recombination event occurred at the junction of open reading frames one and two (ORF1 and ORF2), but this finding was not proven. Norovirus ORF1 encodes nonstructural proteins, including the RNA-dependent RNA polymerase, ORF2 encodes the capsid protein, and ORF3 encodes a small capsid protein (1). Nucleotide sequence of the polymerase and capsid junction generally is conserved among the human norovirus genotypes (4,6), which likely facilitates a recombination event when nucleic acid sequences of parental strains come into physical contact in infected cells, e.g., during copy choice recombination (9).

The Study

We used genetic analysis to investigate a novel, naturally occurring recombinant sapovirus. Two strains were used for the analysis, Mc10 strain (GenBank accession no. AY237420), isolated from an infant hospitalized with acute gastroenteritis in Chiang Mai, Thailand, in 2000 (5), and C12 strain (AY603425), isolated from an infant with gastroenteritis in Sakai, Japan, in 2001 (unpub. data). Although the original polymerase chain reaction (PCR) primer sets that detected these two strains were different, both were directed toward the conserved 5′ end of the capsid gene and have been shown to detect a broad range of sapovirus sequences in genogroup I (GI) and GII (5,10). For Mc10, primers SV5317 and SV5749 were used; for C12, primers SV-F11 and SV-R1 were used.

The complete genomes for Mc10 and C12 were determined as previously described (6). As shown in Figure 1A, the sapovirus genome has an organization slightly different from that of the norovirus genome. ORF1 encodes nonstructural proteins, polymerase, and the capsid protein, and ORF2 encodes a small protein (1).

Initially, we grouped Mc10 and C12 into two distinct GII clusters (i.e., genotypes), on the basis of their capsid sequences (Figure 2A) and the phylogenetic classification scheme of Okada et al. (10). In addition, the overall genomic nucleotide similarity between Mc10 and C12 was 84.3%, while ORF1 and ORF2 shared 85.5% and 73.3% nucleotide identity, respectively. These results corresponded with the capsid-based grouping shown in Figure 2A. By comparing sequence similarity across the length of the genomes with SimPlot with a window size of 100 (11), we discovered a potential recombination site, where the similarity analysis showed a sudden drop in nucleotide identity after the polymerase region (Figure 1B). Nucleotide sequence analysis of ORF1 less the capsid sequence and the capsid sequence indicated 90.1% and 71.3% nucleotide identity, respectively (Figure 1A). To additionally illustrate the nucleotide identities of ORF1 less the capsid sequence, a phylogenetic tree of polymerase sequences of Mc10, C12, and other available strains was developed (Figure 2B). However, for three strains (Mex14917/00,

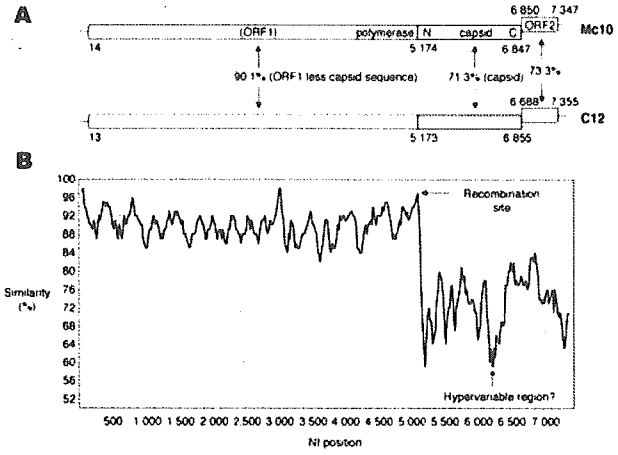

Figure 1. A) The genomic organization of Mc10 and C12 strains. B) the SimPlot analysis of Mc10 and C12. Mc10 genome sequence was compared to C12 by using a window size of 100 bp with an increment of 20 bp. All gaps were removed. The recombination site is suspected to be located between polymerase and capsid genes, as shown by the arrow. The possible hypervariable region for the capsid protein is also shown.

*National Institute of Infectious Diseases, Tokyo, Japan; †Sakai City Institute of Public Health, Sakai, Japan; and ‡University of Tokyo, Tokyo, Japan

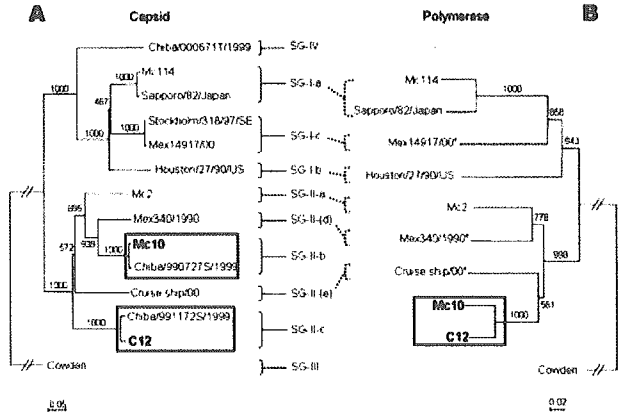

Figure 2. Phylogenetic analysis of (A) capsid (376 nt) and (B) polymerase (289 nt) sequences of Mc10, C12, and additional strains in GenBank. Sapovirus capsid sequences were classified on the basis of the scheme of Okada et al. (10). Two unclassified strains, Mex340/1990 and Cruise ship/00, were assigned SG-II-(d) and SG-II-(e). The asterisks indicate noncontinuous polymerase-capsid sequences. The numbers on each branch indicate the bootstrap values for the genotype. Bootstrap values of >950 were considered statistically significant for the grouping (6). The scale represents nucleotide substitutions per site. GenBank accession no. for the reference strains are as follows: Chiba/000671T/1999, AJ412805; Chiba/990727S/1999, AJ412795; Chiba/991172S/1999, AJ412797; Mc114, AY237422; Cruise ship/00, AY289804 and AY157863; Cowden, AF182760; Houston/27/90/US, U95644; Mc2, AY237419; Mc10, AY237420; Mex340/1990, AF435809 and AF435812; Mex14917/00, AF435813 and AF35810; Sapporo/82/Japan, U65427; and Stockholm/318/97/SE, AF194182.

Mex340/1990, and Cruise ship/00), the polymerase and capsid sequences of ORF1 were not continuous, i.e., they may represent two different strains. Nevertheless, Mc10 and C12 were in the same cluster by polymerase-based grouping but were in distinct clusters by capsid-based grouping (Figure 2). All other strains maintained clusters by polymerase- and capsid-based groupings.

These findings showed Mc10 and C12 had high sequence identity up to the beginning of the capsid region where the sequence identity was considerably lower. These results are easily explained by a recombination event, a single point recombination event occurring at the polymerase-capsid junction. At the end of the polymerase region, there were 44 nt, which included the first 8 nt of the capsid gene and showed 100% homology. After these nucleotides, the identity decreased and was clearly different, as shown in Figure 1B. This conserved region may represent the break and rejoin site for Mc10 and C12 during viral replication, although direct evidence for this event is lacking.

A sudden drop was indicated, followed by a rise in nucleotide identity between nt 6,250 and 6,500 (Figure 1B). Although our initial hypothesis was that another recombination event occurred, closer inspection indicated that this region corresponded to amino acids 358 and 440 for the capsid protein and likely represented the hypervariable region, as described recently in the structural analysis of sapovirus capsid protein (12). For recombinant norovirus strains, we also observed a sudden decrease in nucleotide identity in the related capsid region (13), which represents the outermost protruding domain (P2) and is subject to immune pressure (14). For these reasons, a low homology, even between closely related strains, is generally seen in this region (6), although further studies by sequence analysis with other strains are needed.

In a recent study, we genetically and antigenically analyzed two recombinant norovirus strains (13). When the polymerase-based grouping was performed, these two strains clustered together; when capsid-based grouping was performed, these two strains belonged in two distinct genotypes. When we compared the cross-reactivity of these two viruslike particles (VLPs) and hyperimmune sera against the VLPs, we found distinct antigenic types for the VLPs, although a considerable level of cross-reactivity was found between them. We recently expressed C12 capsid protein that resulted in the formation of VLPs, but we were unsuccessful in expressing Mc10 VLPs (G.S. Hansman, unpub. data); therefore the antigenicity of these two strains remains unknown.

Jiang et al. (4) reported two potential parental norovirus strains that were cocirculating in the same geographic region (Mendoza, Argentina, in 1995), which provides some evidence for where and when the recombination event may have occurred. In addition, Jiang identified the progeny strain from the event, the Arg320 strain. In our study, Mc10 and C12 were isolated from Thailand and Japan, respectively, but we have no evidence for the place and time of the event. While the genetic analysis for Mc10 and C12 identified a possible recombinant sapovirus strain, the analysis does not clarify which of the two strains was the parent strain and which was the progeny strain. Further extensive studies are needed that perform sequence analysis of polymerase and capsid genes and compare results with analysis of other strains. Nevertheless, other strains with capsid sequences that closely match those of Mc10 and C12 are in the public database, which suggests the circulation of other recombinant sapovirus strains.

Conclusions

Recombination and evolution are important survival events for all living creatures as well as viruses. These events in viruses are not completely understood, but they can be potentially dangerous for host species, and they likely influence vaccine designs (15). From our studies, the human sapovirus and norovirus recombination appears limited to the intragenogroup because no intergenogroup

or intergenus recombination has yet been identified and recombination only occurs at the polymerase-capsid junction. Finally, the results of this study have increased our awareness of recombination in the *Sapovirus* genus and may have an influence on the future phylogenetic classification of sapovirus strains.

This work was supported by grants-in-aid from the Ministry of Education, Culture, Sports, Science and Technology of Japan and a Grant for Research on Re-emerging Infectious Diseases from the Ministry of Health, Labor, and Welfare of Japan. G.H. was supported by a PhD scholarship from the Monbusho of Japan.

Dr. Katayama is a senior researcher at National Institute of Infectious Diseases, Tokyo. His research focuses on molecular epidemiologic studies on gastroenteritis viruses and sapovirus and norovirus genome expression.

References

1. Atmar RL, Estes MK. Diagnosis of noncultivatable gastroenteritis viruses, the human caliciviruses. Clin Microbiol Rev. 2001;14:15–37.
2. Noel JS, Fankhauser RL, Ando T, Monroe SS, Glass RI. Identification of a distinct common strain of "Norwalk-like viruses" having a global distribution. J Infect Dis. 1999;179:1334–44.
3. Chiba S, Nakata S, Numata-Kinoshita K, Honma S. Sapporo virus: history and recent findings. J Infect Dis. 2000;181(Suppl 2):S303–8.
4. Jiang X, Espul C, Zhong WM, Cuello H, Matson DO. Characterization of a novel human calicivirus that may be a naturally occurring recombinant. Arch Virol. 1999;144:2377–87.
5. Hansman GS, Katayama K, Maneekarn N, Peerakome S, Khamrin P, Tonusin S, et al. Genetic diversity of norovirus and sapovirus in hospitalized infants with sporadic cases of acute gastroenteritis in Chiang Mai, Thailand. J Clin Microbiol. 2004;42:1305–7.
6. Katayama K, Shirato-Horikoshi H, Kojima S, Kageyama T, Oka T, Hoshino F, et al. Phylogenetic analysis of the complete genome of 18 Norwalk-like viruses. Virology. 2002;299:225–39.
7. Lochridge VP, Hardy ME. Snow Mountain virus genome sequence and virus-like particle assembly. Virus Genes. 2003;26:71–82.
8. Vinje J, Green J, Lewis DC, Gallimore CI, Brown DW, Koopmans MP. Genetic polymorphism across regions of the three open reading frames of "Norwalk-like viruses." Arch Virol. 2000;145:223–41.
9. Worobey M, Holmes EC. Evolutionary aspects of recombination in RNA viruses. J Gen Virol. 1999;80(Pt 10):2535–43.
10. Okada M, Shinozaki K, Ogawa T, Kaiho I. Molecular epidemiology and phylogenetic analysis of Sapporo-like viruses. Arch Virol. 2002;147:1445–51.
11. Lole KS, Bollinger RC, Paranjape RS, Gadkari D, Kulkarni SS, Novak NG, et al. Full-length human immunodeficiency virus type 1 genomes from subtype C-infected seroconverters in India, with evidence of intersubtype recombination. J Virol. 1999;73:152–60.
12. Chen R, Neill JD, Noel JS, Hutson AM, Glass RI, Estes MK, et al. Inter- and intragenus structural variations in caliciviruses and their functional implications. J Virol. 2004;78:6469–79.
13. Hansman G, Doan LP, Kguyen T, Okitsu S, Katayama K, Ogawa S, et al. Detection of norovirus and sapovirus infection among children with gastroenteritis in Ho Chi Minh City, Vietnam. Arch Virol. 2004;149:1673–88.
14. Nilsson M, Hedlund KO, Thorhagen M, Larson G, Johansen K, Ekspong A, et al. Evolution of human calicivirus RNA in vivo: accumulation of mutations in the protruding P2 domain of the capsid leads to structural changes and possibly a new phenotype. J Virol. 2003;77:13117–24.
15. Makeyev EV, Bamford DH. Evolutionary potential of an RNA virus. J Virol. 2004;78:2114–20.

Address for correspondence: Grant S. Hansman, Department of Virology II, National Institute of Infectious Diseases, 4-7-1 Gakuen, Musashimurayama, Tokyo 208-0011, Japan; fax: +81-42-565-3315; email: ghansman@nih.go.jp

Journal of Medical Virology 76:129–136 (2005)

Expression and Antigenicity of Virus-Like Particles of Norovirus and Their Application for Detection of Noroviruses in Stool Samples

Kunio Kamata,[1,2] Kuniko Shinozaki,[3] Mineyuki Okada,[3] Yoshiyuki Seto,[4] Shinichi Kobayashi,[5] Kenji Sakae,[5] Mitsuaki Oseto,[6] Katsuro Natori,[7] Haruko Shirato-Horikoshi,[8] Kazuhiko Katayama,[7] Tomoyuki Tanaka,[8] Naokazu Takeda,[7] and Koki Taniguchi[2]*

[1]*Technical Marketing Department, Denka-Seiken Co., Ltd., Gosen, Niigata, Japan*
[2]*Department of Virology and Parasitology, Fujita Health University School of Medicine, Toyoake, Aichi, Japan*
[3]*Laboratory of Virology, Public Health Laboratory of Chiba Prefecture, Chuoh-ku, Chiba, Japan*
[4]*Department of Virology, Osaka City University Medical School, Abeno-ku, Osaka, Japan*
[5]*Aichi Prefectural Institute of Public Health, Tujimachi, Kita-ku, Nagoya, Japan*
[6]*Ehime Prefectural Institute of Public Health and Environment Science 8-234,Sanbancho, Matsuyama, Ehime, Japan*
[7]*Department of Virology II, National Institute of Infectious Diseases, Musashi-Murayama, Tokyo, Japan*
[8]*Sakai City Institute of Public Health, Sakai, Osaka, Japan*

Human noroviruses (NoVs), members of the genus *Norovirus* in the family *Caliciviridae*, are the leading agents of nonbacterial acute gastroenteritis worldwide. Human NoVs are currently divided into at least two genogroups, genogroup I (GI) and genogroup II (GII), each of which contains at least 14 and 17 genotypes. To explore the genetic and antigenic relationship among NoVs, we expressed the capsid protein of four genetically distinct NoVs, the GI/3 Kashiwa645 virus, the GII/3 Sanbu809 virus, the GII/5 Ichikawa754 virus, and the GII/7 Osaka10-25 virus in baculovirus expression system. An antigen enzyme-linked immunosorbent assay (ELISA) with hyperimmune serum against the four recombinant capsid proteins and characterized previously three capsid proteins derived from GI/1, GI/4, and GII/12 was developed to detect the NoVs antigen in stools. The antigen ELISA was highly specific to the homotypic strains, allowing assignment of a strain to a Norovirus genetic cluster within a genogroup. ***J. Med. Virol. 76:129–136, 2005.*** © 2005 Wiley-Liss, Inc.

KEY WORDS: norovirus; ELISA; gastroenteritis; virus-like particle; calicivirus

INTRODUCTION

Norovirus (NoV), a member of one of four genera in the family *Caliciviridae* [Atmar and Estes, 2001; Green et al., 2001a], is a major cause of water and food-borne acute nonbacterial gastroenteritis, and is composed of many genetically distinct viruses. [Kapikian, 1994; Kapikian et al., 1996; Estes et al., 1997]. The detection and molecular characterization of NoV have been hampered due to the lack of cell culture and small animal models [Duizer et al., 2004]. However, recent progress in molecular cloning and the sequence determination of RNA-dependent RNA polymerase and capsid protein genes of the NoVs has enabled us to classify NoVs into at least two genogroups: genogroup I (GI) and genogroup II (GII) [Green et al., 2001b]. In a previous study, a scheme for genotyping based on the N-terminal capsid protein was demonstrated [Katayama et al., 2002], and a recent report proposed that GI and GII contain at least 14 and 17 genotypes, respectively [Kageyama et al., 2004].

The NoV contains a single-stranded positive-sense RNA genome of 7.6 kb excluding the poly-A tail that encodes three open reading frames (ORFs) [Jiang et al., 1993; Lambden et al., 1993]. ORF1 encodes a nonstructural polyprotein, which is cleaved into functional proteins by a virus-encoded 3C-like protease, and ORF2 and ORF3 encode the major capsid protein VP1 and minor capsid protein VP2, respectively [Jiang et al., 1992; Glass et al., 2000]. When the ORF2 gene alone or the 3′ end of 2.3 kb, including ORF2, ORF3, and the 3′ noncoding region is expressed by a recombinant

Grant sponsor: Ministry of Health, Labor, and Welfare of Japan.

*Correspondence to: Koki Taniguchi, Department of Virology and Parasitology, Fujita Health University School of Medicine, Toyoake, Aichi 470-1192, Japan. E-mail: kokitani@fujita-hu.ac.jp

Accepted 10 January 2005
DOI 10.1002/jmv.20334
Published online in Wiley InterScience (www.interscience.wiley.com)

baculovirus, the recombinant protein spontaneously self-assembles into virus-like particles (VLPs) which are antigenically and morphologically similar to the native virion [Jiang et al., 1992, 2002; Lew et al., 1994a,b; Dingle et al., 1995; Hale et al., 1999; Kobayashi et al., 2000a,b,c; Belliot et al., 2001]. The VLPs have been used successfully for in structural studies [Prasad et al., 1994, 1999], as well as the development of enzyme-linked immunosorbent assay (ELISA) for serological diagnosis of NoV infection [Gray et al., 1993; Green et al., 1993; Parker et al., 1993, 1994, 1995]. Though antigen ELISA using hyperimmune antisera raised against the VLPs has been developed to detect NoV in stools [Graham et al., 1994; Jiang et al., 1995a,b,c; Hale et al., 1999], the sensitivity is low due to the ability of the ELISA to detect only strains closely related to one used to produce the hyperimmune serum [Numata et al., 1994; Jiang et al., 1995a,b,c]. The expression of antigenically distinct more VLPs and the preparation of antisera to them are needed to clarify the antigenic relationship among NoVs.

The expression of four capsid proteins from the GI/3, GII/3, GII/5 and GII/7 NoVs and the preparation of the VLPs are described and the antigenic relationship among seven VLPs, including three NoV VPLs from GI/1, G1/4, and GII/12 prepared previously [Kobayashi et al., 2000a,b,c], and the detection of NoVs in fecal specimens by using an ELISA are described.

MATERIALS AND METHODS

Viruses, RT-PCR, and molecular cloning. Hu/NV/GI/Kashiwa645/1999/JP (Kashiwa645, sequence accession number BD011871), Hu/NV/GII/Sanbu809/1998/JP (Sanbu809, BD011876), and Hu/NV/GII/Ichikawa745/1998/JP (Ichikawa745, BD011877) were associated with outbreaks of acute gastroenteritis as reported by the Kashiwa, Sanbu, and Ichikawa Health Centers in Chiba prefecture, Japan in 1989–1999. Hu/NV/GII/Osaka10-25/1999/JP (Osaka10-25, BD011881) was associated with an outbreak of acute gastroenteritis in Osaka Prefecture, Japan, in 1999. Stool samples containing these viruses were homogenized in phosphate buffered saline (PBS), and a 10% suspension was prepared. After centrifugation at 3,000*g* for 10min, the supernatant was used for RNA extraction with Trizol™ (Gibco BRL, Gaithersburg, MD) [Kobayashi et al., 2000a]. The cDNA synthesis was performed with an oligo-dT15 (Promega Co., Madison, WI) and reverse transcriptase from the Molony murine leukemia virus (Gibco BRL) as described by Green et al. [1997]. An approximately 1.6 kb fragment that encodes the entire VP1 of Kashiwa645, Sanbu809 and Ichikawa745, and a 2.3 kb fragment that encodes the VP1, VP2, 3′ noncoding region, and poly-A of Osaka10-25 were amplified with the primers shown in Table I. The PCR was performed in 100 μl of the reaction mixture containing 2.5 U of Takara Ex Taq (TaKaRa Shuzo Co., Ltd., Kyoto), 10 μl of 10 × PCR buffer, 8 μl of 25 mM dNTPs, 1 μl of 50 μM of each primer, and 5 μl of cDNA. After an initial denaturation at 94°C for 5 min, 35 cycles of amplification were performed using the GeneAmp PCR System 9600 (PE Biosystems, Foster City, CA). Each cycle consisted of denaturation at 94°C for 1 min, primer annealing at 55°C for 1 min, and extension reaction at 72°C for 2 min followed by final extension at 72°C for 7 min. The amplified fragments were cloned into a pCR2.1 plasmid (Invitrogen, San Diego, CA). The nucleotide sequences were determined with an ABI PRISM 310 Genetic Analyzer (Applied Biosystems, Foster City, CA) and phylogenetically analyzed as described previously [Katayama et al., 2002; Kageyama et al., 2004].

Recombinant VLPs

The amplified fragment was isolated from the vector by digestion with the appropriate restriction endonucleases, and inserted into a baculovirus transfer vector pVL1392 (Pharmingen, San Diego, CA), which was used to cotransfect the Sf9 cells (Riken Cell Bank, Tsukuba) with linearized wild-type *Autographa californica* nuclear polyhedrosis virus DNA (Pharmingen) by the lipofectin-mediated method, as described by the manufacturer (Invitrogen). Recombinant baculoviruses thus obtained were selected by two rounds of plaque purification and used to prepare the seed viruses. Tn5 cells (Invitrogen) were infected with the seed virus at a multiplicity of infection (m.o.i.) of 10, incubated at 26.5°C, and the culture medium was harvested at 5–6 days post infection (p.i.). Leupeptin 10 μM (Sigma Chemicals, St. Louis, MO) and 2 μM pepstatin A (Sigma Chemicals) were added to the medium at 3 days p.i. The expression of the recombinant protein in the medium was monitored by sodium dodecyl sulfate-10% polyacrylamide gel electrophoresis (SDS–PAGE) followed by staining with Coomassie brilliant blue. The culture medium was clarified by centrifugation at 10,000*g* for 30 min, and then the VLPs in the supernatant were concentrated by centrifugation at 100,000*g* for 4 hr in a Beckman SW27 rotor. The pellet was resuspended in Grace's medium (DIFCO, Franklin Lakes, New Jersey) and examined by electron microscopy (EM). The VLPs were further purified by $CsCl_2$ equilibrium gradient density gradient centrifugation at 100,000*g* for 24 hr at

TABLE I. Primer Sequences

NoV	Forward primer	Reverse primer
Kashiwa 645	G1/F2 (5′-AATGATGATGGCGTCTAAAGGA-3′)	707R1 (5′-TGAGCCATTATGATCTTCTGATGC-3′)
Sanbu 809	G2/F3 (5′-TTGTGAATGAAGATGGCGTCGA-3′)	MVR1 (5′-AATTATTGAATCCTTCTACGCCCG-3′)
Ichikawa 754	G2/F3 (5′-TTGTGAATGAAGATGGCGTCGA-3′)	SMVR1 (5′-AATTACTGAACCCTTCTACGCCCATTTC-3′)
Osaka 10–25	G2FCR7 (5′-ATGAAGATGGCGTCGAATGACG-3′)	Oligo-dT(33)

16°C. The purified VLPs were used to immunize the animals.

Hyperimmune Sera

Hyperimmune sera to recombinant Kashiwa645 VLPs (r645), Sanbu809 VLPs (r809), Ichikawa754 VLPs (r754), and Osaka10-25 VLPs (r10-25) were prepared in rabbits. The first subcutaneous injection was performed with the purified 500 μg VLPs in Freund's complete adjuvant. After 3 weeks, the animals received two or three booster injections of 250 μg of the VLPs in Freund's incomplete adjuvant at intervals of 1 week. The animals were bled 1 week after the last booster injection. The antibody titers of rabbit hyperimmune sera to VLPs were tested in parallel by an indirect ELISA, as described previously for rSeto 124 VLPs [Kobayashi et al., 2000b] except that a VLP concentration of 0.5 μg/ml was used to coat the ELISA plate. ELISA titers were expressed as the reciprocal of the highest dilution of antiserum giving an optical density (OD) at 450 nm of >0.2.

Antigen ELISA

An antigen detection ELISA was developed using the rabbit hyperimmune sera to four recombinant capsid proteins (r645, r809, r754, and r10–25), and three previously characterized VLPs, Seto 124 VLPs (rSeto) [Kobayashi et al., 2000b], Chiba 407 VLPs (rChiba) [Kobayashi et al., 2000a], and Chitta 1876 VLPs (rChitta) [Kobayashi et al., 2000c]. Microtiter plates (96-well) (Maxisorp, Nunc, Denmark) were coated with 100 μl (0.5 μg of IgG/ml) of the rabbit preimmune (1:8,800 dilution) or hyperimmune sera (1:8,800–12,000 dilutions) in a coating buffer (0.05M carbonate-bicarbonate buffer, pH 9.6) overnight at 4°C. The well was washed twice with PBS containing Tween 20 (PBS-T), and then blocked with 0.5% bovine serum albumin in PBS overnight at 4°C. One-hundred microliter of a 10% stool sample was added to the well and incubated 1 hr at room temperature. After washing the well four times with PBS-T, 100 μl of peroxidase-conjugated rabbit antiserum to VLPs were added to the well and incubated for 1 hr at room temperature. The microplate was washed four times with PBS-T, and then 100 μl of substrate, tetrametyl bentijin (TMB), was added. The plate was left for 30 min at room temperature, and the reaction was stopped with 100 μl of 0.6N H_2SO_4. The OD_{450} value of the reactions at both the hyperimmune and preimmune sera was measured. The sample was considered positive when the difference between the OD_{450} values for the hyperimmune and preimmune sera was >0.15 and the ratio was >2 [Kobayashi et al., 2000c].

Detection of NoV in Stool Specimens by RT-PCR

Extraction of viral RNA from the stools and cDNA synthesis were performed as described above. A forward primer G1F1 and a reverse primer G1R1 were used to amplify the N-terminal VP1 of GI NoV, and a forward primer G2F1 and a reverse primer G2R1 were used to amplify the same region of the GII NoV as previously described [Kobayashi et al., 2000c; Kojima et al., 2002]. The reaction was carried out in 50 μl of the solution containing 1.25 U of Ex Taq polymerase (TaKaRa), 5 μl of 10 × PCR buffer (100 mM Tris-HCl, 15 mM $MgCl_2$, 500 mM KCl), 5 μl of 25 mM deoxynucleotide mixture, 0.5 μM of each primer, and 2 μl of cDNA. After an initial denaturation at 94°C for 5 min, 35 cycles of amplification were performed using the GeneAmp PCR System 9600 (PE Biosystems). The nucleotide sequence and phylogenetic analyses were performed as described above.

Phylogenetic Analysis

Nucleotide sequences of the entire VP1 capsid protein and N-terminal VP1 were aligned with Clustal X (http://www-igbmc.u-strasbg.fr/BioInfo/). The genetic distances were calculated by Kimura's two parameter method [Kimura, 1980], and a distance matrix file was created as described previously [Katayama et al., 2002]. The phylogenetic dendrogram was constructed by the neighbor-joining method [Saitou and Nei, 1987] with 1,000 times of bootstrap resampling [Feisenstein, 1985] as described previously [Katayama et al., 2002].

Genome Sequences

The GenBank accession numbers of the entire VP1 sequences of the strains used in this study are as follows: Aichi124-89 (Seto), accession no. AB031013; Alphatron, AF195847; Amsterdam, AF195848; Appalachicola, AF414406; Arg320, AF190817; Auckland, U46039; M7, AY130761; Birmingham, AJ277612; Boxer, AF538679; Bristol, X76716; BS5, AF093797; Burwash Landing, AF414425; Camberwell, AF145896; Chiba, AB022679; Chitta, AB032758; Desert Shield, U04469; Dijon, AF472623; Erfurt, AF427118; Florida, AF414407; Girlington, AJ277606; Grimsby, AJ004864; Gwynedd, AF414408; Hawaii, U07611; Hillingdon, AJ277607; Honolulu, AF414403; Hesse, AF414406, IdahoFalls, AY054299; Kashiwa47, AB078334; LittleRock; AF414405; Leeds, AJ277608; Manchester, X86560; Mexico, U22498; Melksham, X81879; Miami, AF414410; Musgrove, AJ277614; NewOrleans, AF414422; Norwalk/68, M87661; QueenArms, AJ313030; SaintCloud, AF414427; SaitamaU1, AB039775; SaitamaU16, AB067539; SaitamaU25, AB067543; Saitama SzUG1; AB039774, Seacroft, AJ277620; Sindlesham, AJ277615; Snow Mountain , U70059; Southampton, L07418; Stavanger, AF145709; Toronto, U02030; Valetta, AJ277616; Virginia, AY038599; White River, AF414423; WhiteRose, AJ277610, Winchester, AJ277609; Wortley, AJ277618; Mc37, AY237415, WUG1, AB081723, Kashiwa 645, BD011871, Sanbu 809, BD011876, Ichikawa 754, BD011877, and Osaka 10-25, BD011881.

RESULTS

Characterization of Four NoV Strains

To classify genetically the four NoVs, the entire VP1 genes were amplified by RT-PCR and the nucleotide

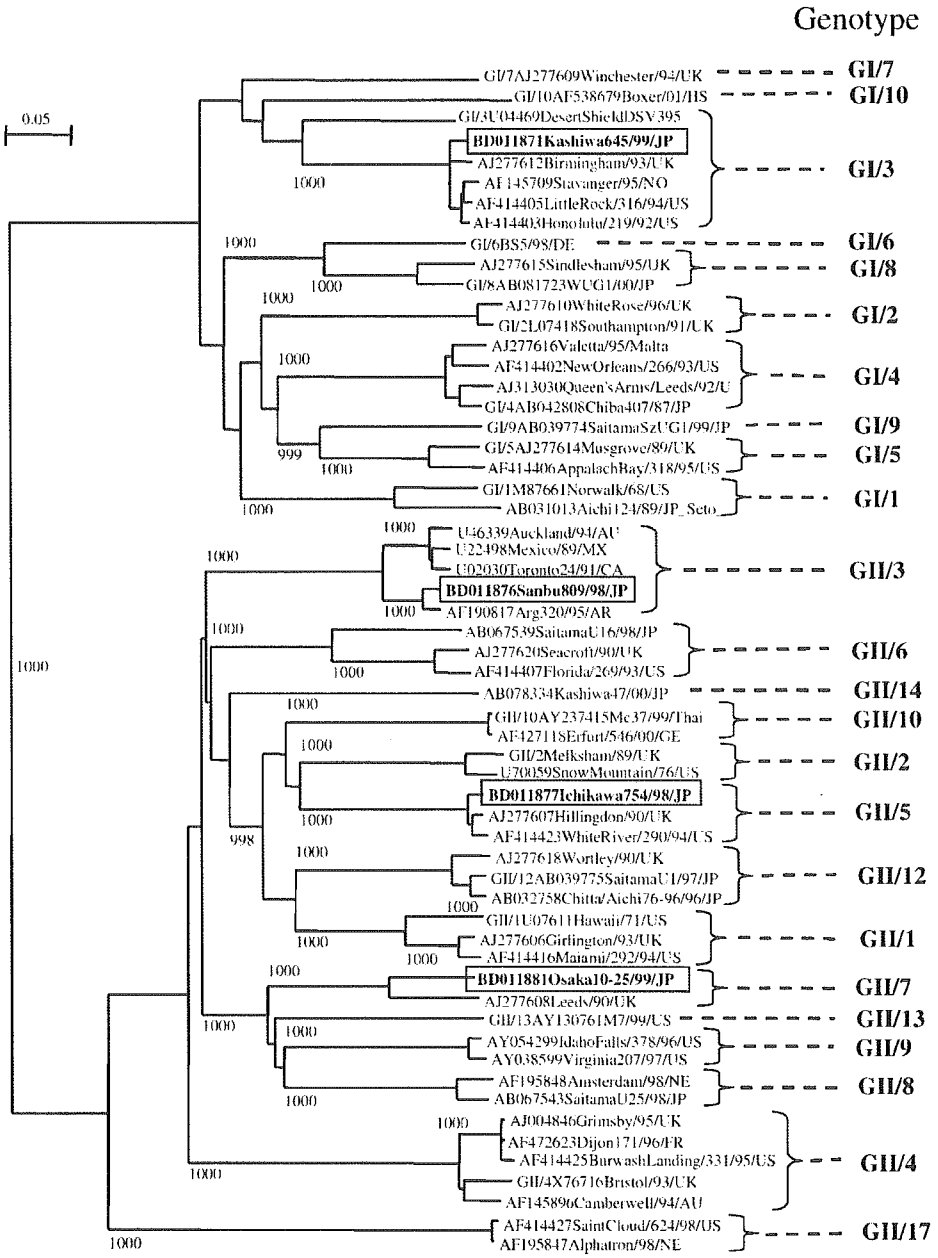

Fig. 1. Phylogenetic tree of NoVs based on entire VP1 nucleotide sequences. The numbers on each branch indicate the bootstrap values for the clusters supported by each branch. Cryptograms indicating the accession number/location or strain name/(isolate)/year/country are given for the strains. Putative genotypes are indicated for each cluster. The names GI/1 to GI/10, and GII/1 to GII/17, with the exception of GII/11, GII/15, and GII/16, are from our previous study [Katayama et al., 2002]. The complete sequences of VP1 of GII/11, GII/15, and GII/16 are not available. The four NoVs characterized in this study are shown in boldface and boxed.

sequence was determined. The phylogenetic analysis of these viruses and representative NoVs is shown in Fig. 1. Kashiwa 645 was close to Birmingham/93/UK and classified into GI/3 where Desert Shield/90/US is the representative strain. The other three strains had higher nucleotide sequence identities to GII than to the GI NoVs. Sanbu 809 was classified into GII/3 with the Toronto/93/CA and Mexico/89/MX viruses. Ichikawa 754 belongs to the GII/5 Hillingdon/90/UK genotype, whereas Osaka 10-25 was classified into GII/7 with the Leeds/90/UK virus.

Expression of the Capsid Proteins in Insect Cells

Tn5 cells (Tn5) were infected with the virus at m.o.i. 10, and the cells were incubated at 26.5°C [Li et al., 1997; Kobayashi et al., 2000a,b,c]. The expressed recombinant proteins were analyzed by 10% SDS–PAGE. A major

protein band with a molecular mass of 58–60 kDa was observed in the infected cells 2 days p.i., and the expression reached to a maximum 6 days p.i. The size of the proteins were in agreement with the molecular mass calculated from the 545, 548, 540, and 541 amino acids of Kashiwa 645, Sanbu 809, Ichikawa 754, and the Osaka 10–25 capsid proteins, respectively. The supernatant was collected at 6 days p.i., centrifuged at 100,000*g* for 2 hr in a Beckman TLA-45 rotor, and then the pellet was examined by EM. Uniform, round-shaped empty VLPs with a 38 nm diameter were observed at over 100 particles per EM field at a magnification of 20,000× (data not shown).

Antigenic Relationships of Newly Expressed Four VLPs With Previously Characterized Three VLPs

Rabbit hyperimmune antisera raised against purified r645, r809, r754, and r10–25 had titers as high as 1:409,600–1:819,200. The hyperimmune serum was not adsorbed with the wild baculovirus-infected Tn5 cell lysate, because the OD values in the antibody ELISA were negligible even when 0.5 μg protein/ml of the lysate was used to coat the microplate wells (data not shown).

The antigenic relationship of the four NoV strains was examined with three previously characterized VLPs (Table II). The highest antibody titers were detected in hyperimmune sera against homologous recombinant capsid antigens for all seven strains. Although variable cross-reactivity was detected among different recombinant antigens, higher cross-reactivity was observed with the intra-genogroup strains than with the inter-genogroup strains. For example, GI Kashiwa 645 is genetically closer to two GI NoVs, Seto 124, and Chiba 407, than the other four GII NoVs. The anti-r645 hyperimmune serum had higher antibody titers to rSeto and rChiba than to the other four GII VLPs. The hyperimmune sera to rSeto and rChiba also had higher antibody titers to the other two GI VLPs than to the other four GII VLPs. Conversely, the four GII NoVs were genetically closer to each other than to the three GI NoVs, and each GII hyperimmune serum had a higher antibody titer to the other three GII VLPs. Thus, NoVs in the same genogroup were not only genetically but also antigenically closer to one another than to those in the different genogroup.

To test further the specificity of hyperimmune serum to seven recombinant capsid proteins, an antigen ELISA was developed. In this experiment, hyperimmune sera (50 ng/well) were used to coat microplate wells to capture the recombinant VLPs. As shown in Table III, the OD values in the homologous reaction decreased in a dose-dependent manner. Little cross-reactions between different genotypes were observed. In contrast, high sensitivity was found in the homologous reactions although the limit of detection is 0.4 ng/ml as observed in the reaction with rChiba and r809, and this corresponds to 2.5×10^6 particles of NoVs.

Detection of NoV Antigen in Stool Specimens

To test the performance of the antigen ELISA, NoVs detection was carried out with stool specimens from acute gastroenteritis patients. Microplates were coated with the rabbit preimmune or hyperimmune sera to capture the antigen in the stool specimens, and peroxidase-conjugated antiserum was used as the detector antibody. In control experiments, antisera against recombinant VLPs efficiently captured at least 4 ng of the homologous antigen but not the heterologous antigen (Table III). The preimmune sera did not capture any of the VLPs at any concentration (the OD value was usually less than 0.05). Two to three representative stool specimens were selected from outbreaks associated with the GI/1, GI/3, GI/4, GII/3, GII/5, GII/7, and GII/12 genotypes to evaluate the antigen ELISA. All specimens were positive by RT-PCR targeting the N-terminal capsid region, and the amplified fragments were genotyped by sequencing analyses followed by phylogenetic analyses (Table IV). All hyperimmune sera except GI/1 Seto reacted only to the homologous genotype samples. In Seto virus detection, all three GI/3 and one of the three GI/4 samples were positive by ELISA. Interestingly, stool samples 98-MC4 (GI/1) and 2000K-518 (GI/3) were negative by EM but positive by the ELISA, suggesting that the antigen ELISA established in this study is capable of detecting disrupted NoV

TABLE II. ELISA Titers of Seven Hyperimmune Antisera Against VLPs

VLPs[a]		Hyperimmune sera against VLP antigens						
		GI/1 Seto	GI/3 645	GI/4 Chiba	GII/3 809	GII/5 754	GII/7 10–25	GII/12 Chitta
GI/1	rSeto	**819200**[b]	25600	12800	200	12800	1600	3200
GI/3	r645	102400	**819200**	25600	400	12800	6400	6400
GI/4	rChiba	102400	25600	**819200**	800	6400	6400	6400
GII/3	r809	25600	6400	6400	**819200**	51200	51200	25600
GII/5	r754	25600	6400	3200	25600	**819200**	25600	51200
GII/7	r10-25	12800	12800	6400	25600	51200	**819200**	25600
GII/12	rChitta	25600	1600	1600	25600	51200	25600	**409600**

[a]Four VLPs: r645, r809, r754, and r10-25 and their hyperimmune sera were prepared in this study, and three VLPs: rSeto, rChiba, and rChitta and their hyperimmune sera were prepared in our previous studies[Kobayashi et al., 2000a,b,c].
[b]ELISA titers were expressed as the reciprocal of the highest dilution of antiserum giving an optical density (OD) at 450 nm of >0.2. Homologous titers are shown in boldface.

TABLE III. Reactivity Between VLPs and Hyperimmune Antisera as Determined by Antigen ELISA

VLPs (ng/mL)		Hyperimmune sera						
		GI/1 Seto	GI/3 645	GI/4 Chiba	GII/3 809	GII/5 754	GII/7 10–25	GII/12 Chitta
rSeto	40	**4.007**	0.075	0.063	0.011	0.010	0.012	0.011
	4	**1.430**	0.034	0.023	0.009	0.011	0.014	0.010
	0.4	0.192	0.028	0.023	0.009	0.010	0.013	0.011
	0	0.010	0.028	0.013	0.008	0.011	0.012	0.011
r645	40	0.173	**3.235**	0.047	0.009	0.014	0.010	0.020
	4	0.061	**0.893**	0.035	0.010	0.010	0.009	0.013
	0.4	0.023	0.114	0.010	0.009	0.011	0.010	0.013
	0	0.010	0.030	0.010	0.009	0.014	0.010	0.015
r Chiba	40	0.105	0.034	**4.259**	0.009	0.012	0.010	0.011
	4	0.048	0.029	**1.408**	0.010	0.011	0.013	0.010
	0.4	0.011	0.026	**0.209**	0.010	0.010	0.010	0.010
	0	0.011	0.026	0.026	0.009	0.011	0.010	0.010
r809	40	0.060	0.028	0.023	**3.650**	0.075	0.056	0.066
	4	0.018	0.031	0.010	**1.271**	0.029	0.023	0.024
	0.4	0.013	0.034	0.007	**0.209**	0.015	0.013	0.014
	0	0.012	0.032	0.010	0.008	0.012	0.010	0.016
r754	40	0.011	0.030	0.025	0.014	**3.994**	0.041	0.083
	4	0.010	0.028	0.024	0.010	**1.329**	0.020	0.039
	0.4	0.010	0.029	0.025	0.010	0.184	0.012	0.015
	0	0.011	0.031	0.025	0.009	0.011	0.010	0.016
r10–25	40	0.018	0.049	0.025	0.016	0.107	**4.326**	0.100
	4	0.015	0.048	0.027	0.011	0.049	**1.343**	0.058
	0.4	0.010	0.038	0.025	0.010	0.017	0.160	0.021
	0	0.010	0.037	0.027	0.010	0.010	0.011	0.010
r Chitta	40	0.014	0.034	0.030	0.011	0.061	0.019	**3.356**
	4	0.011	0.031	0.026	0.010	0.022	0.012	**0.819**
	0.4	0.013	0.032	0.025	0.009	0.013	0.012	0.124
	0	0.014	0.024	0.024	0.009	0.012	0.011	0.025

The reaction was considered to be positive when the difference between the OD_{450} values for the hyperimmune and preimmune sera was >0.15 and the ratio was >2. Positive reactions were shown in boldface.

TABLE IV. Detection of NoV Antigens in Fecal Specimens by Antigen ELISA

Fecal Samples	Hyperimmune sera							EM	RT-PCR	Genotype
	GI/1 Seto	GI/3 645	GI/4 Chiba	GII/3 809	GII/5 754	GII/7 10–25	GII/12 Chitta			
2000K-600	**1.921**[a]	0.052	0.028	0.015	0.013	0.016	0.014	N/A[b]	+	GI/1
98-MC3	**1.407**	0.155	0.060	0.023	0.017	0.018	0.018	+	+	GI/1
98-MC4	**0.596**	0.086	0.056	0.029	0.017	0.018	0.017	–	+	GI/1
2000K-514	**0.498**	**1.521**	0.035	0.029	0.015	0.017	0.017	+	+	GI/3
2000K-518	**0.225**	**0.597**	0.033	0.017	0.012	0.015	0.016	–	+	GI/3
Se1	**0.450**	**2.641**	0.029	0.016	0.012	0.015	0.015	N/A	+	GI/3
2000K-691	0.038	0.040	**0.446**	0.017	0.013	0.015	0.015	+	+	GI/4
2000K-694	**0.358**	0.080	**4.899**	0.049	0.016	0.016	0.017	+	+	GI/4
96-844	0.166	0.071	**2.171**	0.017	0.014	0.015	0.017	+	+	GI/4
98K-826	0.022	0.051	0.065	**1.369**	0.016	0.039	0.066	+	+	GII/3
98K-836	0.018	0.037	0.032	**1.296**	0.015	0.042	0.030	+	+	GII/3
98-249	0.016	0.063	0.030	**1.083**	0.020	0.043	0.034	+	+	GII/3
95-277	0.016	0.034	0.023	0.015	**1.696**	0.024	0.029	+	+	GII/5
00-683	0.011	0.036	0.031	0.090	**0.428**	0.012	0.018	+	+	GII/5
00-684	0.012	0.025	0.015	0.039	**2.994**	0.041	0.136	+	+	GII/5
S99-75	0.037	0.041	0.071	0.101	0.147	**0.426**	0.168	N/A	+	GII/7
S99-21	0.008	0.021	0.035	0.021	0.082	**1.712**	0.010	N/A	+	GII/7
98-41	0.021	0.035	0.031	0.023	0.013	0.028	**1.433**	+	+	GII/12
98-2345	0.019	0.037	0.026	0.020	0.013	0.023	**0.453**	+	+	GII/12
99-1007	0.021	0.055	0.036	0.130	0.014	0.031	**2.722**	+	+	GII/12

[a]The reaction was considered to be positive when the difference between the OD_{450} values for the hyperimmune and preimmune sera was >0.15 and the ratio was >2. Positive reactions were shown in boldface.
[b]Not applicable.

antigen, although the titers were relatively low even in the homologous reaction. Another possible (even more likely) explanation is that the antigen ELISA is more sensitive than EM as described previously [Graham et al., 1994].

DISCUSSION

This study describes the cloning, sequencing, and expression of the capsid proteins of four currently circulating NoV strains and their genetic and antigenic relationships with three previously characterized strains. The phylogenetic analyses indicated that these seven strains belong to GI/1, GI/3, GI/4, GII/3, GII/5, GII/7, and GII/12. In contrast to the rapid accumulation of information for genetic diversity, at least 14 in the GI and 17 in the GII genotypes, studies on the determination of antigenic type have been relatively slow [Kageyama et al., 2004]. This is because generation of the VLPs antigen is not an easy task, and a comparative study with a panel of a large number of VLPs antigens and their antisera is difficult to be performed at the moment. Continued preparation and characterization of more VLPs antigens and their hyperimmune sera are highly useful to refine the panel.

Although the seven antigenic types were distinguishable by the hyperimmune antisera generated against the VLPs, low levels of cross-reaction were observed among these strains when the antibody ELISA was used. Because no NoV specific antibody was detected in the preimmune animal sera, the cross-reactive antibodies in the hyperimmune antisera originated from common antigenic epitopes among NoVs. In fact, Kitamoto et al. [2002] obtained not only genogroup-specific, but also common cross-reactive monoclonal antibodies (MAbs) for four GI and six GII VLPs. Further characterization of antigenic epitopes using MAbs for the antigenic type-specific diagnosis of NoV is needed. In antibody ELISA (Table II), higher responses were observed between the intra-genogroup strains than between the inter-genogroup strains. This observation is worth noting, because it indicates that GI and GII are not only genetically, but also antigenically distinct.

Previous observations of the immune responses of patients involved in outbreaks have also explained the common antigenic epitopes. Immune responses to multiple antigenic types, most of which were caused by a single NoV strain, are often detected in outbreaks of gastroenteritis [Vipond et al., 2004]. Higher responses to homotypic than to heterotypic strains may allow us to make a seroresponse-based diagnosis of NoV infection. Indeed, we recently identified a GII/4 infection in a hospital based on the immune responses of the patients (data not shown).

As has been shown in the case of the Norwalk virus, Mexico virus, Grimsby virus, Seto virus, Chiba virus, and Chitta virus, the antigen ELISA for NoV was highly genotype-specific [Numata et al., 1994; Hale et al., 1996, 1999; Kobayashi et al., 2000a,b,c]. Further generation of VLPs antigens and hyperimmune sera against each genotype VLPs and the subsequent development of both antibody and antigen ELISAs are necessary for the detection of NoVs, for the antigenic relationship among NoVs, and for the classification of NoVs.

ACKNOWLEDGMENTS

This work was supported in part by a grant for Research on Emerging and Re-emerging Infectious Diseases, a grant for Special Research, a grant for Research on Food Safety, and a grant for Research on Health Sciences focusing on Drug Innovation from the Ministry of Health, Labor, and Welfare of Japan.

REFERENCES

Atmar RL, Estes MK. 2001. Diagnosis of noncultivatable gastroenteritis viruses, the human caliciviruses. Clin Microbiol Rev 14: 15–37.

Belliot G, Noel JS, Li JF, Seto Y, Humphrey CD, Ando T, Glass RI, Monroe SS. 2001. Characterization of capsid genes, expressed in the baculovirus system, of three new genetically distinct strains of "Norwalk-like viruses." J Clin Microbiol 39:4288–4295.

Dingle KE, Lambden PR, Caul EO, Clarke IN. 1995. Human enteric Caliciviridae: The complete genome sequence and expression of virus-like particles from a genetic group II small round structured virus. J Gen Virol 76:2349–2355.

Duizer E, Schwab KJ, Neill FH, Atmar RL, Koopmans MP, Estes MK. 2004. Laboratory efforts to cultivate noroviruses. J Gen Virol 85:79–87.

Estes MK, Atmar RL, Hardy ME. 1997. Norwalk and related diarrhea viruses. In: Richmann DD, Whitley RJ, Hayden FG, editors. Clinical virology. New York: Churchill Livingstone, Inc. pp 1073–1095.

Feisenstein J. 1985. Confidence limits on phylogenies: An approach using the bootstrap. Evolution 39:783–791.

Glass PJ, White LJ, Ball JM, Leparc-Goffart I, Hardy ME, Estes MK. 2000. Norwalk virus open reading frame 3 encodes a minor structural protein. J Virol 74:6581–6591.

Graham DY, Jiang X, Tanaka T, Opekun AR, Madore HP, Estes MK. 1994. Norwalk virus infection of volunteers: New insights based on improved assays. J Infect Dis 170:34–43.

Gray JJ, Jiang X, Morgan-Capner P, Desselberger U, Estes MK. 1993. Prevalence of antibodies to Norwalk virus in England: Detection by enzyme-linked immunosorbent assay using baculovirus-expressed Norwalk virus capsid antigen. J Clin Microbiol 31:1022–1025.

Green KY, Lew JF, Jiang X, Kapikian AZ, Estes MK. 1993. Comparison of the reactivities of baculovirus-expressed recombinant Norwalk virus capsid antigen with those of the native Norwalk virus antigen in serologic assays and some epidemiologic observations. J Clin Microbiol 31:2185–2191.

Green SM, Lambden PR, Caul EO, Clarke IN. 1997. Capsid sequence diversity in small round structured viruses from recent UK outbreaks of gastroenteritis. J Med Virol 52:14–19.

Green KY, Ando T, Balayan MS, Clarke IN, Estes MK, Matson DO, Nakata S, Neill JD, Studdert MJ, J TH. 2001a. Caliciviridae. In: van Regenmortel MHV, Fauquet CM, Bishop DHL, Carsten EB, Estes MK, Lemon SM, Maniloff J, Maya MA, McGeoch DJ, Pringle CR, Wickner RB, editors. Virus taxonomy. 3rd edn, San Diego: Academic Press, Inc. pp 725–734.

Green KY, Chanock RM, Kapikian AZ. 2001b. Human caliciviruses. In: Knipe DM, Howley PM, Griffin DE, editors. Fields virology, 4th edn, Philadelphia: Lippincott Williams & Wilkins. pp 841–874.

Hale AD, Lewis D, Green J, Jiang X, Brown DWG. 1996. Evaluation of an antigen capture ELISA based on recombinant Mexico virus capsid protein. Clin Diagn Virol 5:27–35.

Hale AD, Crawford SE, Ciarlet M, Green J, Gallimore C, Brown DW, Jiang X, Estes MK. 1999. Expression and self-assembly of Grimsby virus: Antigenic distinction from Norwalk and Mexico viruses. Clin Diagn Lab Immunol 6:142–145.

Jiang X, Wang M, Graham DY, Estes MK. 1992. Expression, self-assembly, and antigenicity of the Norwalk virus capsid protein. J Virol 66:6527–6532.

Jiang X, Wang M, Wang K, Estes MK. 1993. Sequence and genomic organization of Norwalk virus. Virology 195:51–61.

Jiang X, Cubitt D, Hu J, Dai X, Treanor J, Matson DO, Pickering LK. 1995a. Development of an ELISA to detect MX virus, a human calicivirus in the snow mountain agent genogroup. J Gen Virol 76:2739–2747.

Jiang X, Matson DO, Ruiz-Palacios GM, Hu J, Treanor J, Pickering LK. 1995b. Expression, self-assembly, and antigenicity of a snow mountain agent-like calicivirus capsid protein. J Clin Microbiol 33:1452–1455.

Jiang X, Wang J, Estes MK. 1995c. Characterization of SRSVs using RT-PCR and a new antigen ELISA. Arch Virol 140:363–374.

Jiang X, Zhong WM, Farkas T, Huang PW, Wilton N, Barrett E, Fulton D, Morrow R, Matson DO. 2002. Baculovirus expression and antigenic characterization of the capsid proteins of three Norwalk-like viruses. Arch Virol 147:119–130.

Kageyama T, Shinohara M, Uchida K, Fukushi S, Hoshino FB, Kojima S, Takai R, Oka T, Takeda N, Katayama K. 2004. Co-existence of multiple genotypes, including newly identified genotypes, in outbreaks of Norovirus gastroenteritis. J Clin Microbiol 42:2988–2995.

Kapikian AZ. 1994. Norwalk and Norwalk-like viruses. In: Kapikian AZ, editor. Viral infections of the gastroentestinal tract. 2nd edn, New York: Marcel Dekker, Inc. pp 471–518.

Kapikian AZ, Estes MK, Chanock RM. 1996. Norwalk group of viruses. In: Fields BN, Knipe DM, Howley PM, Chanock RM, Melnick JL, Monath TP, Roizmann B, Straus SE, editors. Fields virology. 3rd edn, Philadelphia, PA: Lippincott–Raven Publishers. pp 783–810.

Katayama K, Shirato-Horikoshi H, Kojima S, Kageyama T, Oka T, Hoshino F, Fukushi S, Shinohara M, Uchida K, Suzuki Y, Gojobori T, Takeda N. 2002. Phylogenetic analysis of the complete genome of 18 Norwalk-like viruses. Virology 299:225–239.

Kimura M. 1980. A simple method for estimating evolutionary rates of base substitutions through comparative studies of nucleotide sequences. J Mol Evol 16:111–120.

Kitamoto N, Tanaka T, Natori K, Takeda N, Nakata S, Jiang X, Estes MK. 2002. Cross-reactivity among several recombinant calicivirus virus-like particles (VLPs) with monoclonal antibodies obtained from mice immunized orally with one type of VLP. J Clin Microbiol 40:2459–2465.

Kobayashi S, Sakae K, Natori K, Takeda N, Miyamura T, Suzuki Y. 2000a. Serotype-specific antigen ELISA for detection of Chiba virus in stools. J Med Virol 62:233–238.

Kobayashi S, Sakae K, Suzuki Y, Shinozaki K, Okada M, Ishiko H, Kamata K, Suzuki K, Natori K, Miyamura T, Takeda N. 2000b. Molecular cloning, expression, and antigenicity of Seto virus belonging to genogroup I Norwalk-like viruses. J Clin Microbiol 38:3492–3494.

Kobayashi S, Sakae K, Suzuki Y, Ishiko H, Kamata K, Suzuki K, Natori K, Miyamura T, Takeda N. 2000c. Expression of recombinant capsid proteins of chitta virus, a genogroup II Norwalk virus, and development of an ELISA to detect the viral antigen. Microbiol Immunol 44:687–693.

Kojima S, Kageyama T, Fukushi S, Hoshino FB, Shinohara M, Uchida K, Natori K, Takeda N, Katayama K. 2002. Genogroup-specific PCR primers for detection of Norwalk-like viruses. J Virol Methods 100:107–114.

Lambden PR, Caul EO, Ashley CR, Clarke IN. 1993. Sequence and genome organization of a human small round-structured (Norwalk-like) virus. Science 259:516–519.

Lew JF, Kapikian AZ, Jiang X, Estes MK, Green KY. 1994. Molecular characterization and expression of the capsid protein of a Norwalk-like virus recovered from a Desert Shield troop with gastroenteritis. Virology 200:319–325.

Lew JF, Kapikian AZ, Valdesuso J, Green KY. 1994. Molecular characterization of Hawaii virus and other Norwalk-like viruses: Evidence for genetic polymorphism among human caliciviruses. J Infect Dis 170:535–542.

Li TC, Yamakawa Y, Suzuki K, Tatsumi M, Razak MA, Uchida T, Takeda N, Miyamura T. 1997. Expression and self-assembly of empty virus-like particles of hepatitis E virus. J Virol 71:7207–7213.

Numata K, Nakata S, Jiang X, Estes MK, Chiba S. 1994. Epidemiological study of Norwalk virus infections in Japan and Southeast Asia by enzyme-linked immunosorbent assays with Norwalk virus capsid protein produced by the baculovirus expression system. J Clin Microbiol 32:121–126.

Parker S, Cubitt D, Jiang JX, Estes M. 1993. Efficacy of a recombinant Norwalk virus protein enzyme immunoassay for the diagnosis of infections with Norwalk virus and other human "candidate" caliciviruses. J Med Virol 41:179–184.

Parker SP, Cubitt WD, Jiang XJ, Estes MK. 1994. Seroprevalence studies using a recombinant Norwalk virus protein enzyme immunoassay. J Med Virol 42:146–150.

Parker SP, Cubitt WD, Jiang X. 1995. Enzyme immunoassay using baculovirus-expressed human calicivirus (Mexico) for the measurement of IgG responses and determining its seroprevalence in London, UK. J Med Virol 46:194–200.

Prasad BV, Rothnagel R, Jiang X, Estes MK. 1994. Three-dimensional structure of baculovirus-expressed Norwalk virus capsids. J Virol 68:5117–5125.

Prasad BV, Hardy ME, Dokland T, Bella J, Rossmann MG, Estes MK. 1999. X-ray crystallographic structure of the Norwalk virus capsid. Science 286:287–290.

Saitou N, Nei M. 1987. The neighbor-joining method: A new method for reconstructing phylogenetic trees. Mol Biol Evol 4:406–425.

Vipond IB, Caul EO, Hirst D, Carmen B, Curry A, Lopman BA, Pead P, Pickett MA, Lambden PR, Clarke IN. 2004. National epidemic of Lordsdale Norovirus in the UK. J Clin Virol 30:243–247.

JOURNAL OF VIROLOGY, Feb. 2006, p. 1513–1523 Vol. 80, No. 3
0022-538X/06/$08.00+0 doi:10.1128/JVI.80.3.1513–1523.2006

High-Resolution Molecular and Antigen Structure of the VP8* Core of a Sialic Acid-Independent Human Rotavirus Strain†

Nilah Monnier,[1,2] Kyoko Higo-Moriguchi,[3] Zhen-Yu J. Sun,[4] B. V. Venkataram Prasad,[5] Koki Taniguchi,[3] and Philip R. Dormitzer[2,6]*

Harvard College, Cambridge, Massachusetts 02138[1]; Laboratory of Molecular Medicine, Children's Hospital, Boston, Massachusetts 02115[2]; Department of Virology and Parasitology, Fujita Health University School of Medicine, Toyoake, Aichi 470-1192, Japan[3]; Department of Biological Chemistry and Molecular Pharmacology, Harvard Medical School, Boston, Massachusetts 02115[4]; Verna and Marrs McLean Department of Biochemistry and Molecular Biology, Baylor College of Medicine, One Baylor Plaza, Houston, Texas 77030[5]; and Department of Pediatrics, Harvard Medical School, Boston, Massachusetts 02115[6]

Received 22 July 2005/Accepted 25 October 2005

The most intensively studied rotavirus strains initially attach to cells when the "heads" of their protruding spikes bind cell surface sialic acid. Rotavirus strains that cause disease in humans do not bind this ligand. The structure of the sialic acid binding head (the VP8* core) from the simian rotavirus strain RRV has been reported, and neutralization epitopes have been mapped onto its surface. We report here a 1.6-Å resolution crystal structure of the equivalent domain from the sialic acid-independent rotavirus strain DS-1, which causes gastroenteritis in humans. Although the RRV and DS-1 VP8* cores differ functionally, they share the same galectin-like fold. Differences between the RRV and DS-1 VP8* cores in the region that corresponds to the RRV sialic acid binding site make it unlikely that DS-1 VP8* binds an alternative carbohydrate ligand in this location. In the crystals, a surface cleft on each DS-1 VP8* core binds N-terminal residues from a neighboring molecule. This cleft may function as a ligand binding site during rotavirus replication. We also report an escape mutant analysis, which allows the mapping of heterotypic neutralizing epitopes recognized by human monoclonal antibodies onto the surface of the VP8* core. The distribution of escape mutations on the DS-1 VP8* core indicates that neutralizing antibodies that recognize VP8* of human rotavirus strains may bind a conformation of the spike that differs from those observed to date.

Rotavirus is the most important cause of severely dehydrating childhood gastroenteritis worldwide (37). To prime the nonenveloped virion for host membrane penetration, intestinal trypsin cleaves the rotavirus spike protein, VP4, into two fragments, VP8* and VP5* (15). In some strains, VP8* mediates initial attachment to target cells by binding cell surface sialic acid (SA) (6, 16). In electron cryomicroscopy image reconstructions of trypsin-primed, SA-dependent virions, the protruding part of the spikes has approximate twofold symmetry (Fig. 1). It is tipped by paired heads, separated by a small gap (41, 44). The heads are formed by a globular domain of VP8* (14). We refer to this globular domain as the "VP8* core," because it remains intact following limit protease digestion of recombinant VP4 (12). VP5* forms more virion-proximal parts of the spikes (Fig. 1) and has a hydrophobic apex (13), which has been implicated as a potential membrane penetration region (32). VP8* masks the hydrophobic apex of VP5* on primed spikes (13). During cell entry, VP8* probably separates from VP5*, exposing the hydrophobic apex and allowing a fold-back rearrangement of VP5*. Some antibodies that bind VP8* appear to neutralize virus by triggering uncoating—the shedding of VP4 or its fragments and the coat protein VP7 (45). This mechanism of neutralization suggests that conformational changes involving VP8* could trigger subsequent entry events, such as VP5* rearrangement and outer-layer disassembly. VP8* may also function intracellularly, binding intracellular tumor necrosis factor receptor-associated factors to activate cellular signaling pathways (28).

Although SA was the first rotavirus receptor identified (2), most rotavirus strains do not, in fact, bind this receptor during entry (6). None of the strains that are known to be virulent in humans bind SA (6). Differences between SA-dependent and SA-independent strains extend beyond the ability or inability of their spike proteins to bind SA: SA-independent strains are generally more fastidious in cell culture than SA-dependent strains (40, 42), and although SA-independent strains infect polarized epithelial cells from either the apical or basolateral membrane, SA-dependent strains enter only at the apical surface (4).

The VP8* core is an important target of neutralizing antibodies against rotavirus (reviewed in reference 14). Some neutralizing monoclonal antibodies (MAbs) that recognize this domain on SA-dependent strains protect mouse pups from rotavirus diarrhea when present in the gut lumen (33). The VP8* core is the major determinant of P serotype (which correlates reasonably well with P genotype) for both SA-dependent and SA-independent strains (22). Therefore, this domain contains key neutralization determinants for both functional variants. While most VP4-specific MAbs that neutralize SA-dependent rotavirus virions map to the VP8* fragment, most VP4-specific MAbs that neutralize SA-independent virions map to the VP5* fragment (reviewed in reference 25). It is not known whether this difference reflects biological differences between SA-dependent and SA-

* Corresponding author. Mailing address: Laboratory of Molecular Medicine, Enders 673, Children's Hospital, Boston, MA 02115. Phone: (617) 355-3026. Fax: (617) 730-1967. E-mail: dormitze@crystal.harvard.edu.

† Supplemental material for this article may be found at http://jvi.asm.org.

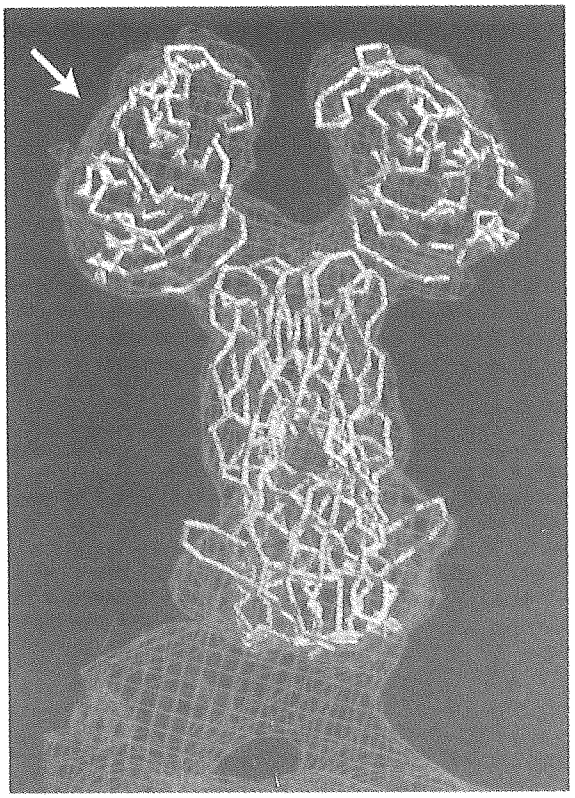

FIG. 1. The rotavirus VP4 spike. The Cα traces of the VP8* core (white) and a globular domain of VP5* (yellow) from RRV are fitted to the molecular envelope of the VP4 spike in an approximately 12-Å-resolution electron cryomicroscopy image reconstruction of a primed SA11-4F rotavirus virion. The arrow indicates the perspective of the depictions in Fig. 3 and 4B.

independent strains or the use of different strategies to screen hybridomas.

Although understanding the structure and function of SA-independent strains is particularly important for understanding and preventing rotavirus gastroenteritis in humans, SA-independent strains are less studied than SA-dependent strains. X-ray crystal and nuclear magnetic resonance (NMR) solution structures of the VP8* core of an SA-dependent simian rotavirus strain (RRV) have been obtained (14), but neither electron cryomicroscopy-based image reconstructions nor high-resolution structures are available for any SA-independent strain. Therefore, the structural basis for the differences in VP8* function is not known. Here, we present the X-ray crystal structure of the VP8* core from rotavirus strain DS-1, an SA-independent P genotype 4 strain that causes gastroenteritis in humans. We also report neutralization escape mutations of VP8* selected by two human monoclonal antibodies derived from cDNA of B lymphocytes from naturally infected humans. Mapping neutralization escape mutations onto the DS-1 VP8* core structure suggests that VP8*-specific antibodies that neutralize SA-dependent and SA-independent rotavirus strains recognize different conformations of the spike protein.

MATERIALS AND METHODS

Subcloning of the DS-1 and KU VP8* cores. Genes encoding the VP8* cores of rotavirus strains DS-1 and KU were subcloned from recombinant baculoviruses that contain the full-length DS-1 and KU VP4 coding sequences (18). Primers to amplify the KU VP8* coding sequence were designed based on a previously banked KU VP4 sequence (GenBank accession code M21014). The sequence of the DS-1 VP8* core was determined from DNA amplified by PCR from the recombinant baculovirus using primers complementary to sequences in the BlueBac2 vector on either side of the VP4 coding sequence. The sequences encoding KU and DS-1 VP4 residues 60 to 223 (the VP8* cores) were isolated as PCR products with XhoI and NotI ends and with a potential trypsin cleavage site just N terminal to residue 60. Each fragment was subcloned into the multiple cloning site of a pGex 4T-1 vector (Amersham Biosciences) that had been digested with SalI and NotI.

Expression and purification of recombinant VP8* cores. The RRV, DS-1, and KU VP8* cores were expressed in *Escherichia coli* strain BL21 and purified as described previously (14). Overnight cultures were diluted 1:100 in LB containing 0.1 mg/ml ampicillin and incubated at 37°C. When the cultures reached an A_{600} of about 0.6, the temperature was reduced to 25°C. After 30 to 60 min of incubation at 25°C, isopropyl-β-D-thiogalactopyranoside (IPTG) was added to 1 mM. The cultures were then incubated for an additional 4 h at 25°C before being harvested. Pelleted bacteria were lysed by sonication. The lysates were clarified by centrifugation in a Ti45 rotor (Beckman) at 40,000 rpm for 2 h at 4°C. The clarified lysates were passed over a glutathione-Sepharose column (Amersham Biosciences), and the VP8* cores were cleaved from the bound glutathione *S*-transferase (GST) tags by incubation on the column with 5 μg/ml tosylsulfonyl phenylalanyl chloromethyl ketone-treated trypsin (Worthington Biochemical) in TNC (20 mM Tris, pH 8.0, 100 mM NaCl, 1 mM $CaCl_2$) for 2 h at room temperature. The trypsin was removed from the released VP8* by passage over a benzamidine-Sepharose column (Amersham Biosciences), and any residual tryptic activity was eliminated by the addition of 1 mM phenylmethylsulfonyl fluoride and 2.5 mM benzamidine. The VP8* cores were further purified by size exclusion chromatography on a Superdex 200 column (Amersham Biosciences) in TNE (20 mM Tris, pH 8.0, 100 mM NaCl, 1 mM EDTA) at 4°C using a fast-protein liquid chromatography system (Amersham Biosciences).

Crystallization. The DS-1 VP8* core crystallized in space group P1 with the following unit cell parameters: a = 42.42 Å, b = 84.12 Å, c = 90.77 Å, α = 90.03°, β = 90.02°, and γ = 75.54°. The crystals have a solvent content of 38.5%, and each asymmetric unit contains eight VP8* cores. Crystals formed within 1 week at 20°C in hanging drops, with a sample solution containing 5 to 10 mg/ml protein in TNE-0.02% sodium azide-0.1 mM benzamidine, mixed 1:1 with a well solution containing 20% polyethylene glycol 4000, 500 mM sodium chloride, 100 mM sodium citrate, pH 5.6, and 3% ethanol or ethylene glycol. Harvested crystals were soaked in a cryoprotectant solution containing 22% polyethylene glycol 4000, 550 mM sodium chloride, 100 mM sodium citrate, pH 5.6, 3% ethanol or ethylene glycol, 15% glycerol and then frozen by rapid immersion in liquid nitrogen.

X-ray diffraction data collection and processing. X-ray diffraction data were collected at 100 K and a wavelength of 0.916 Å using beam line F1 at the Cornell High Energy Synchrotron Source. Diffracted X rays were detected by an ADSC Quantum 4 charge-coupled device. Diffraction data were indexed, integrated, and scaled using HKL2000 (HKL Research, Inc.). (For scaling statistics, see Table 2.)

Structure determination and refinement. The DS-1 VP8* core structure was determined by molecular replacement, using an initial phasing model based on the previously determined structure of the SA-bound RRV VP8* core (14). Rotation and translation solutions were determined using CNS (3). The structure was refined by multiple cycles of simulated annealing, energy minimization, and individual B-factor refinement using CNS (3). The model was rebuilt in O (24) using simulated annealing omit maps calculated in CNS (3) to eliminate phasing bias from the molecular replacement model. The geometry of the structures was analyzed using PROCHECK (29). (For refinement statistics, see Table 2.)

NMR spectroscopy. Purified protein for NMR was prepared as described above, except that size exclusion chromatography was carried out in 20 mM sodium phosphate, pH 7.0–100 mM NaCl, and the resulting protein sample was dialyzed into 20 mM sodium phosphate, pH 7.0–10 mM NaCl. The assayed peptide was ^{15}N labeled on valine and had the sequence TVEPVS, corresponding to DS-1 VP4 residues 60 to 64 plus a C-terminal serine. To avoid competition between the peptide and residues of the authentic N-terminal leader of the unlabeled DS-1 VP8* core, residues 60 to 64 of the core were mutated to SGSGG using PCR. Samples were made 10% in D_2O for field locking. Spectra were obtained at 25°C using a 500-MHz Bruker spectrometer equipped with a cryoprobe. Two-dimensional ^{15}N-^{1}H heteronuclear single quantum coherence spectra showed no change in the chemical shifts of the ^{15}N valines of the peptide when 0.29 mM DS-1 VP8* core was mixed with 0.1 mM peptide. NMR data were processed using PROSA (20), and spectra were analyzed using XEASY (1).

Structural analysis and figure production. Structure alignments were calculated using LSQKAB in CCP4 (7). Amino acid variability was calculated by AMAS (30). To determine the accessibility of VP8* core surfaces for antibody binding on trypsin-primed virions, the DS-1 VP8* core structure was aligned with an RRV VP8* core structure that had been fitted to an approximately 12-Å electron cryomicroscopy-based envelope of trypsin-primed SA11-4F rotavirus particles, contoured at 0.5 σ, as previously described (13). The envelope and fitted crystal structure were probed with the crystal structure of an Fab of a human immunoglobulin G1(κ) in complex with Lewis Y nonoate methyl ester (Protein Data Bank accession code 1CLY) using O (23, 24). Residues that could be brought into contact with any portion of the antigen-combining site were scored as accessible. The figures were made using GRASP (34), MOLSCRIPT (27), Illustrator (Adobe Systems, Inc.), and Photoshop (Adobe Systems, Inc.).

Selection of neutralization escape mutants. Rotavirus strain KU (30 μl; 3.6×10^5 PFU) was pretreated with trypsin (10 μg/ml) and mixed with 70 μl of purified 1-2H (200 μg/ml) or 2-3E (50 μg/ml) Fab in Eagle's minimum essential medium (MEM). After 1 h of incubation at 37°C, the virus-antibody mixtures were inoculated onto MA104 cell monolayers in 1 ml of Eagle's MEM in roller tubes (15 mm by 15 cm). After adsorption for 1 h, the monolayers were washed with phosphate-buffered saline and then incubated in a rotator (RT-550; Taitec Inc.) with 1 ml of Eagle's MEM containing purified 1-2H (100 μg/ml) or 2-3E (25 μg/ml) antibody and trypsin (5 μg/ml). Cultures were harvested 7 days after infection. After three rounds of propagation in the presence of neutralizing antibody, the selected viruses were plaque purified on CV-1 cells.

Sequencing of rotavirus variants. Full-length cDNA encoding VP4 and VP7 was prepared by reverse transcription-PCR. Nucleotide sequences were determined directly from the PCR products using ABI Prism BigDye Terminator Cycle Sequencing Ready Reaction Kits (PE Biosystems) with an automated sequencer, the ABI Prism 310 Genetic Analyzer (PE Applied Biosystems). The VP4-encoding genes of the two selected viruses each differed from the parental gene by a single nucleotide substitution. The VP7-encoding genes contained no mutations.

Protein structure and nucleotide sequence accession numbers. The atomic coordinates and structure factor amplitudes for the DS-1 VP8* core have been deposited in the Protein Data Bank under accession code 2AEN. Nucleotide sequences have been deposited in GenBank with the following accession codes: DS-1 VP8* core, DQ141310; KU VP4 clone 1, AB222784; M-KU-1-2H, AB222785; M-KU-2-3E, AB222786.

RESULTS AND DISCUSSION

Expression, purification, and stability of rotavirus VP8* cores. The VP8* core is a compact domain that presents conformational neutralizing epitopes. Our previously reported data demonstrate that the RRV VP8* core (P genotype 3) can be expressed in *E. coli* as a soluble GST fusion protein (14). After glutathione affinity chromatography, the domain can be separated from its GST tag by trypsin cleavage and purified by size exclusion chromatography with high yield as a homogeneous, protease-resistant, and very soluble protein (14).

We tested whether the VP8* core of an SA-independent strain that causes gastroenteritis in humans has similarly favorable characteristics. When expressed and purified using the protocol developed for the RRV VP8* core, the DS-1 VP8* core (P genotype 4) was obtained in good yield as a homogeneous, protease-resistant, soluble, pure protein (Fig. 2A and Table 1). As assayed by size exclusion chromatography, sodium dodecyl sulfate-polyacrylamide gel electrophoresis (SDS-PAGE), matrix-assisted laser desorption ionization mass spectrometry, and N-terminal sequencing, the RRV and DS-1 VP8* cores remain intact, homogeneous, and soluble after storage at 4°C for approximately 2 years (Fig. 2A, Table 1, and data not shown).

This purification procedure is also effective at producing a homogeneous VP8* core from a P genotype 8, SA-independent rotavirus strain, KU (Fig. 2B and Table 1). Together, P genotypes 4 and 8 cause more than 90% of human cases of rotavirus gastroenteritis in temperate climates (11). Although the KU VP8* core is also very soluble, it is produced in relatively low yield and undergoes substantially more degradation and aggregation with storage than do the RRV and DS-1 VP8*

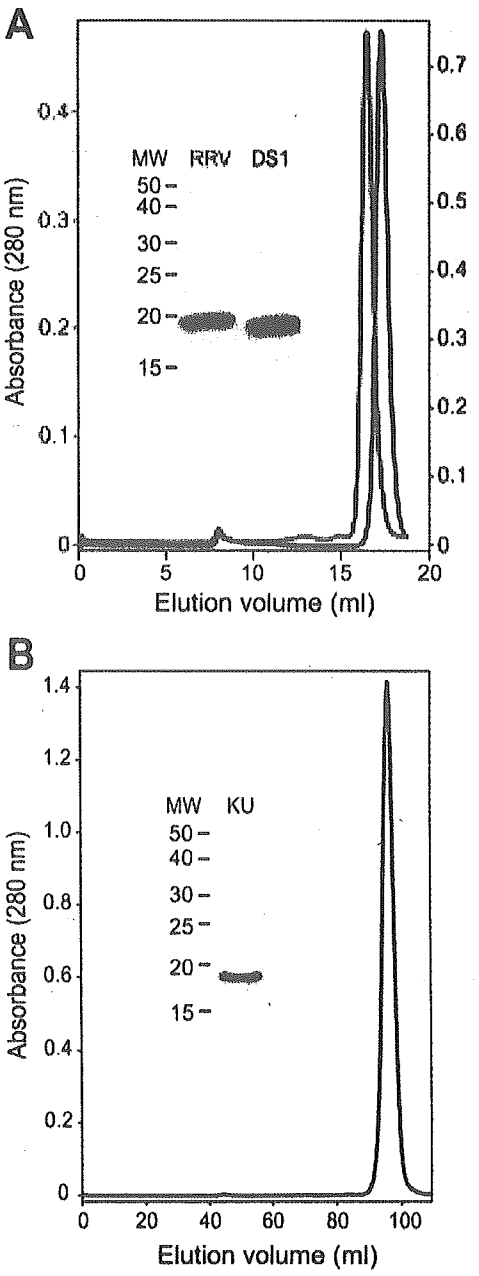

FIG. 2. Size exclusion chromatography and SDS-PAGE of purified VP8* cores. (A) Chromatograms of RRV (red) and DS-1 (blue) VP8* cores, which were separated on a Superdex 200 10/30 column at 4°C in TNE after storage for 2 years at 4°C in TNE with 0.02% sodium azide and 0.1 mM benzamidine. The inset image of a Coomassie blue-stained SDS-PAGE gel shows stored samples prior to chromatography. (B) Chromatogram of a freshly prepared sample of the KU VP8* core, which was separated on a Hi-Load Superdex 200 16/60 column at 4°C in TNE. The inset image of a Coomassie-blue stained SDS-PAGE gel shows protein from the pooled peak fractions. Apparent molecular masses that correspond to peak elution volumes are listed in Table 1.

TABLE 1. Biochemical characteristics of the RRV, DS-1, and KU VP8* cores

Characteristic	Value		
	RRV	DS-1	KU
No. of rotavirus VP4 residues in construct	60–224	60–223	60–223
Predicted MW	18570.6	18758.3	18882.4
MW fresh[a]	18592.8	18826.8	19104.4
MW after storage[a]	18568.2	18734.3	Multiple fragments
Length of storage (days)	798	718	767
Apparent mass (kDa)[b]	23.6 (after storage)	17.4 (after storage)	7.9 (fresh)[c]
Yield (mg/liter of bacterial culture)[d]	16	8.6	2.6
Solubility (mg/ml)	≥88	≥39.1	≥22.7

[a] Determined by matrix-assisted laser desorption ionization mass spectrometry.
[b] Based on elution volume by gel filtration chromatography (Fig. 2).
[c] This anomalously low apparent molecular mass probably results from affinity of the KU VP8* core for the chromatography medium.
[d] Yield refers to the final purified VP8* core.

cores (Fig. 2B, Table 1, and data not shown). Thus, the biochemical characteristics of the RRV and DS-1 VP8* cores make them promising potential immunogens for use in recombinant rotavirus vaccines. The less favorable characteristics of the KU VP8* core indicate that developing an antigenic cocktail of VP8* cores to completely cover the P types causing human disease will require screening of additional strains and possibly protein engineering.

Structural comparison of the DS-1 and RRV VP8* cores. Using the X-ray crystal structure of the RRV VP8* core as an initial phasing model for molecular replacement, we determined the X-ray crystal structure of the DS-1 VP8* core at 1.6-Å resolution (see Materials and Methods) (Table 2). The DS-1 VP8* core, like the RRV VP8* core, resembles the galectins, a family of animal lectins, in its fold. It is built around a central β-sandwich, with a β-hairpin (strands E and F) packed against a six-stranded β-sheet and a C-terminal α-helix packed against a five-stranded β-sheet (Fig. 3A). Each asymmetric unit contains eight molecules of the DS-1 VP8* core. There are no major conformational differences between the eight molecules, which can be superimposed on each other with an average root mean square deviation (RMSD) between Cα atoms of 0.26 Å (not shown).

Although the DS-1 and RRV VP8* cores have only 45% amino acid identity (for residues 65 to 224 of RRV and 65 to 223 of DS-1), they can be superimposed on each other with an RMSD of 1.04 Å for 159 equivalent Cα atoms (Fig. 3B). The broad surface that is formed by the EF β-hairpin, strands H and G of the six-stranded β-sheet, and strands J and K of the five-stranded β-sheet is furrowed by two clefts (Fig. 3A to D). Both clefts are wider in the DS-1 VP8* core than in the RRV VP8* core (Fig. 3B). In the DS-1 VP8* core, the architecture of the cleft corresponding to the RRV SA binding site, which lies between the five-stranded and six-stranded β-sheets, is extensively reworked (Fig. 3C to F). In the RRV VP8* core, the R101 side chain amide makes key contacts with SA. It projects from strand D to the floor of the binding site to form a positively charged surface patch and makes bidentate hydrogen bonds to the glycerol group of the bound carbohydrate (Fig. 3D and F). In the DS-1 VP8* core, phenylalanine replaces arginine at this site and has a very different structural role. F101 of DS-1 makes no contribution to the molecular surface (Fig. 3C); instead, its aromatic ring forms part of a hydrophobic core in the interface between the β-sheets (Fig. 3E). In the RRV VP8* core, the aromatic rings of Y155 and Y188 project out into solvent to form walls on either side of the SA binding pocket (Fig. 3D and F). In the DS-1 VP8* core, replacement of these residues by R154 and S187 removes these walls. In fact, the R154 side chain replaces the floor of the SA binding pocket with a low ridge, as it stretches across the gap between the six- and five-stranded β-sheets (Fig. 3C and E). Although the structural data do not exclude the possibility that an alternative carbohydrate ligand binds in place of SA in

TABLE 2. Crystallographic data collection and refinement statistics

Statistic	Value
Data collection	
Resolution limit (Å)	1.6
No. of unique reflections	153,466
Redundancy[a]	1.95 (1.72)
Completeness[a] (%)	96.8 (94.7)
I/σ[a]	17.2 (3.4)
R_{sym}[a,b] (%)	5.0 (37.6)
Refinement	
No. of polypeptide chains	8
No. of protein atoms	10,762
No. of water molecules	1,724
No. of glycerol molecules	6
No. of ethanol molecules	4
No. of amino acids with alternative conformations	43
Residues in allowed regions of Ramachandran plot (%)	100
Residues in most favored regions of Ramachandran plot (%)	91.8
RMSD bond lengths (Å)	0.011
RMSD bond angles (°)	1.31
Mean B value (Å^2)	24.91
RMSD main chain B (Å^2)	1.019
Resolution range (Å)	14.9–1.6
R factor[c]	0.158
Free R factor[c]	0.192

[a] Value for the highest-resolution shell is given in parentheses.
[b] $R_{sym} = \Sigma(I - \langle I \rangle)/\Sigma I$. $\langle I \rangle$ is the average intensity over symmetry-equivalent reflections.
[c] R factor = $(\Sigma||F_{obs}| - |F_{calc}||)/\Sigma|F_{obs}|$, where the summations is over the working set of reflections. For the free R factor, the summation is over the test set of reflections (5% of the total reflections).

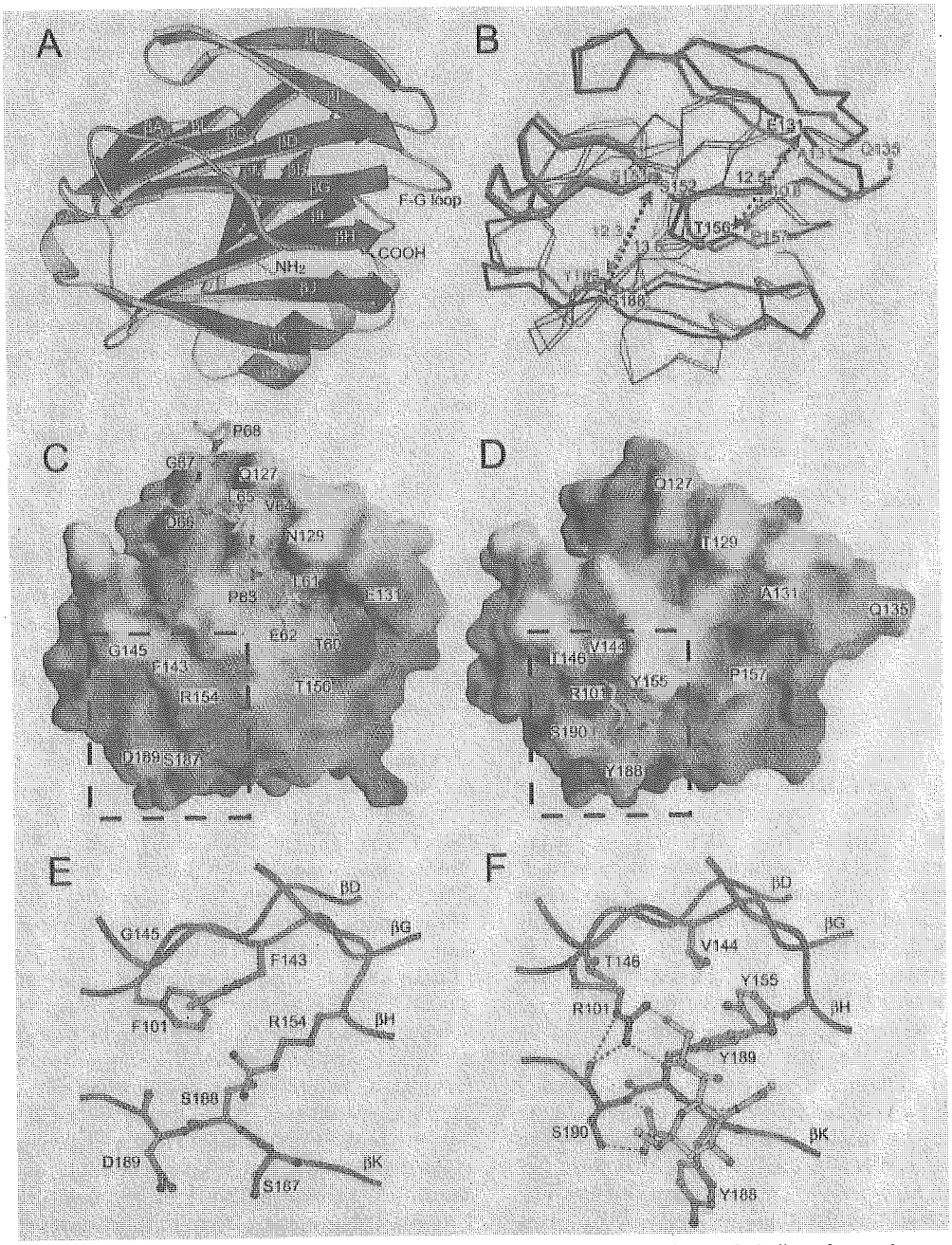

FIG. 3. Comparison of DS-1 and RRV VP8* cores. (A) Ribbon diagram of the DS-1 VP8* core. Labeling of secondary-structure elements is as previously described for the RRV VP8* core (14), except that strand βH, which splits into strands βH and βH′ in RRV, is continuous in DS-1. The EF β-hairpin is red, the six-stranded β-sheet is green, and the five-stranded β-sheet is blue. (B) Superimposed Cα traces of the DS-1 VP8* core (blue) and the RRV VP8* core (red). Residue Q135 of RRV, which lacks a structural equivalent in DS-1, is indicated. The blue and red arrows indicate the widths of surface clefts, measured in Å between Cα atoms of the labeled residues, for the DS-1 and RRV VP8* cores, respectively. (C) Surface representation of the DS-1 VP8* core colored by electrostatic potential. Blue is positive; red is negative. The bound leader of an adjacent molecule in the crystal is depicted with a ball-and-stick model. Residues in the space-filling model are labeled in white text boxes. Residues in the ball-and-stick model are labeled in yellow text boxes. (D) Surface representation of the RRV VP8* core colored by electrostatic potential. The bound sialoside is depicted with a ball-and-stick model. (E) Molecular details of the site in DS-1 VP8* that corresponds to the RRV SA binding pocket. The depicted area is indicated by the dashed outline in panel C. (F) Molecular details of the SA binding pocket of RRV VP8*. The depicted area is indicated by a dashed outline in panel D. Selected hydrogen bonds are indicated by dashed gray lines. In panels E and F, residues on strand βK are depicted with backbone and side chain atoms; only Cα and side chain atoms of other residues are shown. The perspective of all the panels is indicated by the arrow in Fig. 1.

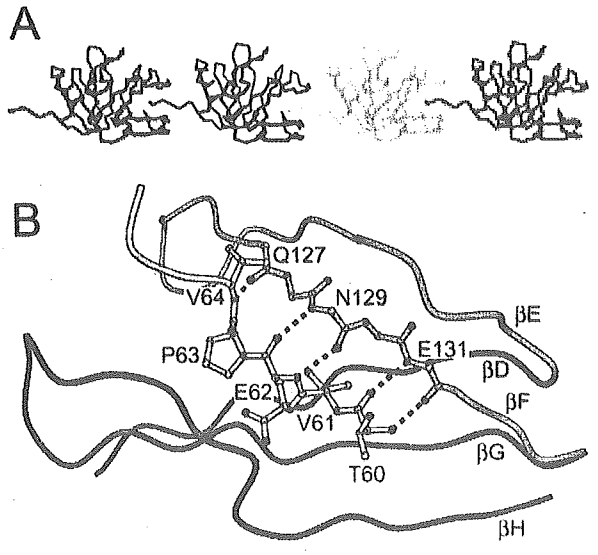

FIG. 4. Leader binding in the DS-1 VP8* core crystal. (A) Cα traces of representative molecules in the crystal. The cleft between the β-hairpin and the six-stranded β-sheet of each molecule binds the leader of an adjacent molecule. (B) Molecular details of the cleft-to-leader interaction. The leader is depicted in yellow. Hydrogen bonds are depicted as dotted black lines. Residues on strand βF are depicted without side chains. The perspective and coloring match Fig. 3A.

DS-1, the surface of the DS-1 VP8* core that corresponds to the RRV SA binding site is not an obvious binding pocket.

DS-1 VP8* binds a polypeptide chain in a second surface cleft. Does the DS-1 VP8* core structure suggest an alternative ligand to SA? The packing of the EF β-hairpin against the six-stranded β-sheet creates a cleft, which is adjacent to the cleft between the β-sheets that forms the SA binding pocket in RRV (Fig. 3A, C, and D). In the DS-1 VP8* core crystal, this cleft is occupied by the five N-terminal residues (residues 60 to 64) of an adjacent molecule, so that each DS-1 VP8* core "bites its neighbor's tail," linking the cores into chains (Fig. 4A). The bound N-terminal residues are not part of the tightly folded structure of the core, but instead form an extended N-terminal "leader." The equivalent residues are disordered in the RRV VP8* core crystal and solution structures (14). In the DS-1 VP8* core crystal, this leader is held in alignment by five backbone amide-to-carbonyl hydrogen bonds that form between residues 60, 62, and 64 of the leader and residues 131, 129, and 127 of strand F in the β-hairpin, thus making a new intermolecular three-stranded β-sheet with strands E and F (Fig. 4B). Leader binding is also stabilized by insertion of the aliphatic V61 side chain into a pocket lined by hydrophobic residues at the base of the cleft (Fig. 5B).

We used NMR spectroscopy to assay the binding in solution of a peptide based on the DS-1 VP8* core leader sequence to this potential peptide binding cleft (see Materials and Methods). The free peptide did not bind in the cleft with measurable affinity (data not shown). Close inspection of the DS-1 VP8* core crystal structure indicates that the bound leader does not fit the cleft optimally: the cleft continues beyond the N terminus of the bound leader (Fig. 3C), the hydrophobic pocket that holds the V61 side chain could accommodate a bulkier moiety (not shown), the P63 side chain prevents formation of potential hydrogen bonds between the leader and residues in strand H and the GH loop (Fig. 4B), and the leader is forced out of the cleft C terminal to P63 by steric hindrance from the tightly folded region of its own VP8* core (Fig. 4A).

The peptide binding cleft of the DS-1 core is one of the only exposed VP8* core surfaces that is conserved among SA-independent strains (Fig. 5B), suggesting a conserved function. A similar, but narrower, cleft is also present on the surface of the RRV VP8* core (Fig. 3D). Similar residues line this cleft in SA-dependent and SA-independent strains (see Table S1 in the supplemental material). Fitting to electron cryomicroscopy image reconstructions of virions from SA-dependent strains shows that this cleft is exposed at the tips of the VP4 spikes in a position favoring interaction with host cell proteins (Fig. 5B and D). As described previously, the VP8* β-hairpin appears to be an elaboration of a much shorter loop in the galectins, and it blocks the galectin carbohydrate binding site (14). The DS-1 VP8* core crystal structure suggests that this elaboration of the β-hairpin may also have created a new ligand binding site at the tip of the primed VP4 spike.

Structural polymorphism. Many rotavirus strains, such as DS-1, have a deletion in the FG loop (Table 3) so that they lack a residue that is structurally equivalent to RRV residue Q135 (Fig. 3B). The FG loop links the EF β-hairpin to the six-stranded β-sheet (Fig. 3A). Near the deletion, the potential peptide binding cleft between the EF β-hairpin and the six-stranded β-sheet is wider in the DS-1 VP8* core than in the RRV VP8* core (Fig. 3B), possibly because the shorter loop does not permit as close an approximation of the proximal portion of the β-hairpin to the six-stranded β-sheet.

Most human rotavirus strains have this deletion in the FG loop (Table 3). The infrequently isolated human rotavirus strains without the deletion have P types (such as 5A[3], 3[9], 4[10], and 11[14]), that also include animal rotavirus strains. These strains may have been introduced into human populations relatively recently. The deletion is consistently associated with SA independence (as verified by the presence of a hydrophobic residue at position 101), but it is not required for SA independence (Table 3). The phylogeny of rotavirus VP4 (6) does not clearly demonstrate whether this common structural feature is an adaptation to replication and spread in humans or simply a consequence of common ancestry: the clustering of VP4 molecules with the deletion in a single clade (containing P genotypes 4, 6, 8, and 19) is not absolute, and some bovine strains (in the outlying P[11] group) also have the deletion. Potential ligand binding in the cleft between the β-hairpin and the six-stranded β-sheet suggests that the structural polymorphism may reflect differences in ligand specificity.

Escape mutations selected by human neutralizing MAbs against rotavirus. Three human neutralizing MAbs against rotavirus have been derived from a phage display library of B-lymphocyte cDNA from naturally infected humans (21). The phage antibodies were selected for binding to rotavirus strain KU virions, tested for neutralization of strain KU, and converted to immunoglobulin G1 MAbs through recombinant DNA manipulation. One of the MAbs, 2-11G, binds VP7. The other two bind VP4 and neutralize heterotypically (i.e., neutralize more than one P type): 1-2H neutralizes P[4] and P[8]; 2-3E neutralizes P[6] and P[8].

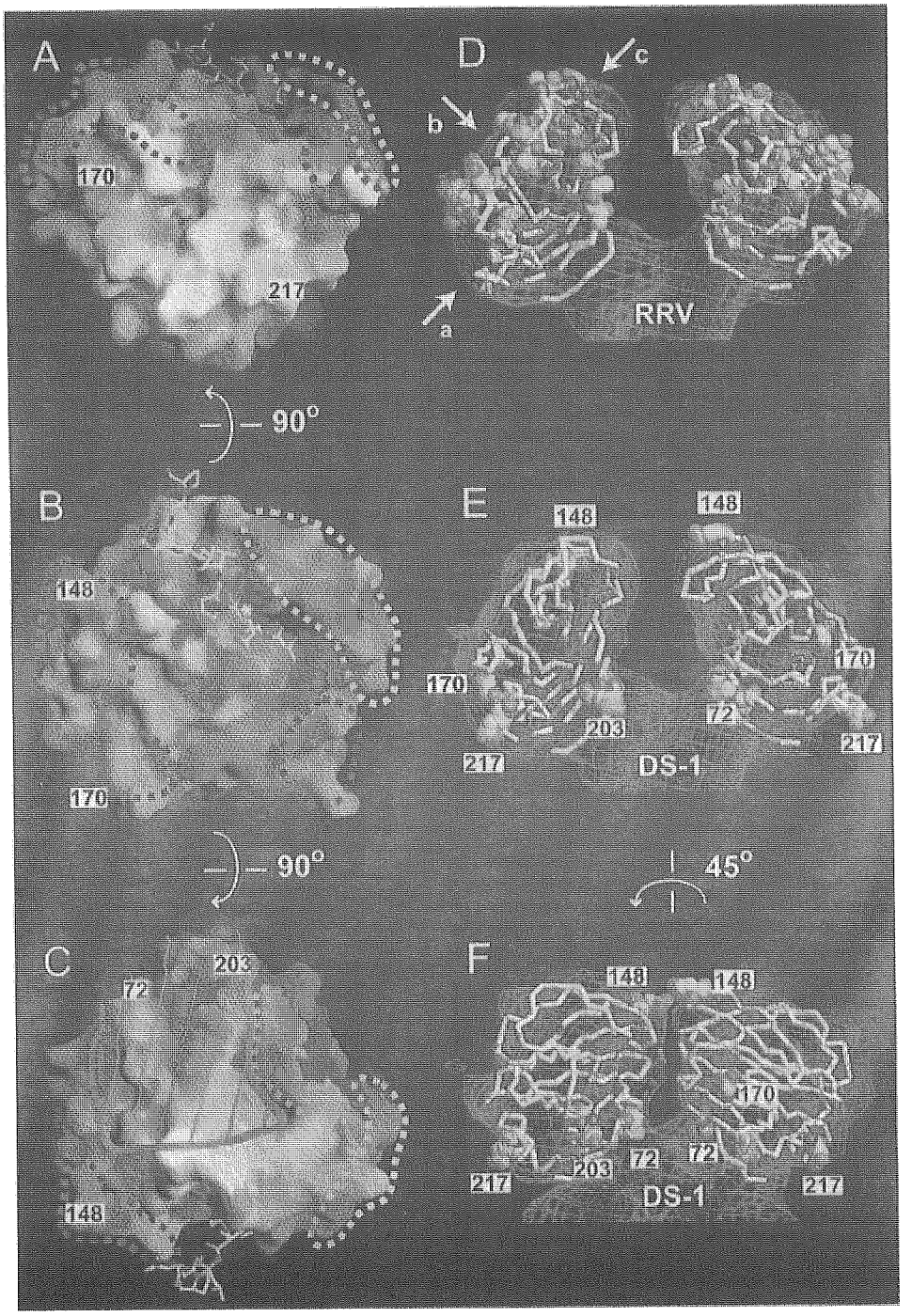

FIG. 5. Neutralization surfaces of the RRV and DS-1 VP8* cores. Panels A to C show three views of a surface representation of the DS-1 VP8* core, colored by conservation among a set of VP8* sequences that contains one representative from each of 14 SA-independent P genotypes (Table 3). Blue is conserved; red is variable. Residue numbers mark neutralization escape mutations selected in SA-independent human rotavirus strains. Dashed outlines mark the previously described (14) neutralization epitopes of SA-dependent strains: green, 8-1; blue, 8-2; yellow, 8-3; pink, 8-4. The white asterisk in panel B indicates a hydrophobic pocket at the base of the peptide binding cleft. Red lines in panel C mark a surface that is inaccessible to antibody binding when the DS-1 VP8* core is fitted to the head of the SA11-4F VP4 spike. The bound leader is depicted with a ball-and-stick model. The perspectives of panels A, B, and C are indicated by arrows a, b, and c, respectively, in panel D. An observer looking down arrow c would be "head down" to view the perspective in panel C. In panels D to F, Cα traces of VP8* cores are fitted to the molecular envelope of the head from an electron cryomicroscopy image reconstruction of the SA11-4F spike on primed virions. Residues selected in neutralization escape mutants are indicated with space-filling models. (D) The RRV VP8* core with escape mutations selected in SA-dependent animal rotavirus strains. (E) The DS-1 VP8* core with escape mutations selected in SA-independent human rotavirus strains. Exposed escape mutations are labeled by residue number. (F) The model from panel E rotated 45° to show more clearly the inaccessible escape mutations in the cleft between the heads.